AD_____

Award Number: DAMD17-01-1-0125

TITLE: The Role of Actin Polymerization in Tumor Metastasis

PRINCIPAL INVESTIGATOR: Xi Zhan, Ph.D.

CONTRACTING ORGANIZATION: American National Red Cross
Rockville, Maryland 20855

REPORT DATE: August 2003

TYPE OF REPORT: Annual

PREPARED FOR: U.S. Army Medical Research and Materiel Command
Fort Detrick, Maryland 21702-5012

REPORT DOCUMENTATION PAGE

Form Approved
OMB No. 074-0188

1. AGENCY USE ONLY (Leave blank)	2. REPORT DATE	3. REPORT TYPE AND DATES COVERED
	August 2003	Annual (1 Aug 2002 - 31 Jul 2003)

4. TITLE AND SUBTITLE
The Role of Actin Polymerization in Tumor Metastasis

5. FUNDING NUMBERS
DAMD17-01-1-0125

6. AUTHOR(S)
Xi Zhan, Ph.D.

7. PERFORMING ORGANIZATION NAME(S) AND ADDRESS(ES)
American National Red Cross
Rockville, Maryland 20855

E-Mail: zhanx@usa.redcross.org

8. PERFORMING ORGANIZATION REPORT NUMBER

9. SPONSORING / MONITORING AGENCY NAME(S) AND ADDRESS(ES)
U.S. Army Medical Research and Materiel Command
Fort Detrick, Maryland 21702-5012

10. SPONSORING / MONITORING AGENCY REPORT NUMBER

11. SUPPLEMENTARY NOTES
Original contains color plates: All DTIC reproductions will be in black and white.

12a. DISTRIBUTION / AVAILABILITY STATEMENT
Approved for Public Release; Distribution Unlimited

12b. DISTRIBUTION CODE

13. ABSTRACT (Maximum 200 Words)
Breast cancer is frequently associate with gene amplification of EMS1 or cortactin, a protein that regulates the assembly of filamentous actin (F-actin). Previous studies have demonstrated that overexpression of cortactin results in increase in metastases and invasion of breast tumor cells. The goal of this project is to reveal the biological significance of the interaction of cortactin with phospholipids, which are known to play a critical role in the modulation of cell migration in response to extracellular stimuli. Cortactin binds to a subset of phosphatidylinositides, including phosphatidylinositol 5-phosphoate (PI(5)P), phosphatidylinoistol 4,5 biophosphoate (PI(4,5)P2) and phosphatidylinositol 4-phosphoate (PI(4)P). Interestingly, not all those phospholipids show a similar effect on the activity of cortactin. While PI(5)P increases the activity of cortactin for actin assembly, PI(4)P inhibits the cortactin mediated actin branching. This data indicates that the activity of cortactin is regulated by different types of membrane phospholipids. In addition, we also utilized small interference RNA to inhibit the expression of cortactin in breast cancer cells. These RNAs inhibit the cortactin expression by more than 80%, impair the actin assembly and reduce the formation of invadopodia. Thus, cortactin is essential for the actin-based invasiveness of tumor cells and modulates actin assembly that is subject to regulation by specific phospholipids.

14. SUBJECT TERMS
Breast cancer

15. NUMBER OF PAGES
26

16. PRICE CODE

17. SECURITY CLASSIFICATION OF REPORT	18. SECURITY CLASSIFICATION OF THIS PAGE	19. SECURITY CLASSIFICATION OF ABSTRACT	20. LIMITATION OF ABSTRACT
Unclassified	Unclassified	Unclassified	Unlimited

Table of Contents

Introduction

Breast cancer is frequently associated with gene amplification of the chromosome 11q13, resulting in overexpression of cortactin, a cortical actin-associated protein and a prominent substrate of protein tyrosine kinase Src. Cortactin is accumulated in peripheral structures of cells including lamellipodia and membrane ruffles where cortical actin is enriched. In MDA-MB-231 breast cancer cells plated on extracellular matrix cortactin is enriched in invadopodia, a type of membrane protrusions that participates in degradation of and invasion into the matrix. While the precise role of cortactin in tumor progression remains unclear, amplification and overexpression of cortactin appear to be intimately associated with patients with poor prognosis or relapse, indicating that overexpression of cortactin may contribute to a late stage of tumor progression. This notion is further strengthened by our recent study showing that MDA-MB-231 cells overexpressing wild-type cortactin acquired higher potential for cell migration in vitro and tumor invasion and metastasis in vivo. The protein sequence of cortactin is featured by six and one half tandem copies of a unique 37-amino-acid repeat and a Src homology 3 (SH3) domain at the carboxyl terminus. Our recent study also demonstrated that cortactin binds via its N-terminus to Arp2/3 complex, a primary machinery for actin polymerization. Such interaction plays a critical role in the regulation of actin cytoskeleton in cell leading edges. Studies from this laboratory have further found that cortactin interacts with a certain type of phosphatidylinositides, which bind to the plasma membrane and are known to be implicated in the regulation of the cytoskeleton. Therefore, we hypothesize that the association of cortactin with these phospholipids may be important for the dynamics of actin cytoskeleton at the cell leading edge and play a role in tumor invasion and metastasis. The project funded by this grant is to characterize the detail of the interaction of cortactin with phospholipids and seek for opportunities by which we may be able to compromise metastasis.

Body

Task: Study the effects of phosphatidylinositides on the activity of cortactin-mediated actin polymerization and structural elements essential for the association of cortactin with phospholipids

The rationale to study cortactin phosphatidylinositide association is to investigate the regulation of the activity of cortactin. While our study in the previous year demonstrated that cortactin binds to multiple types of phospholipids, PI(4)P and PI(5) appeared to be the strongest affinity for cortactin. To define the significance of the binding of these types of lipids on the function of cortactin, we examined the effect of PI(4)P and PI(5)P on the function of cortactin. Synthetic PI(5)P, $PI(4,5)P_2$, PI(4)P (Echelon Biosciences) were suspended in chloroform and transferred to glass vessels. The chloroform was removed by vacuum. The lipid film was resuspended in buffer (10 mM imidazole [pH 7.0], 50 mM KCl, 1 mM EGTA, 1 mM $MgCl_2$) by vortexing in a 37°C water-bath, and subjected to sonication for 10 min. The resulting liposome was added in actin polymerization reaction containing 1.5 μM Mg-ATP G-actin, Arp2/3 complex and cortactin at concentrations as indicated. Pyrene fluorescence was measured at excitation at 365 nm and emission at

407 nm, and the value was collected on a LS50B spectrofluorometer (Perkin Elmer) at a rate of 1 point every 3s. As shown in Figure 1A, the activity of cortactin in the stimulation of Arp2/3 complex for actin polymerization is significantly enhanced by PI(5)P, not by PI(4,5)P_2. Interestingly, PI(4)P inhibits significantly cortactin/Arp2/3 mediated actin assembly at concentration of 100 μM (Figure 1B). The effect of phospholipids on actin branching was also examined (Figure 2). While the actin assembled in the presence of Arp2/3 complex/cortactin or in addition to PI(5)P were significantly branched, those in the presence of PI(4)P were long with little branching. This result indicates specificities of PI(4)P and PI(5)P on cortactin.

In addition, we have established a series of small interference RNA (siRNA) to inhibit the expression of cortactin in MDA-MB-231 cells. Two of these RNAs can effectively knock down cortactin by more than 80%. In a collaboration with Susette Muller in Georgetown, we have found that cortactin siRNA can inhibit invadopodia formation of tumor cells.

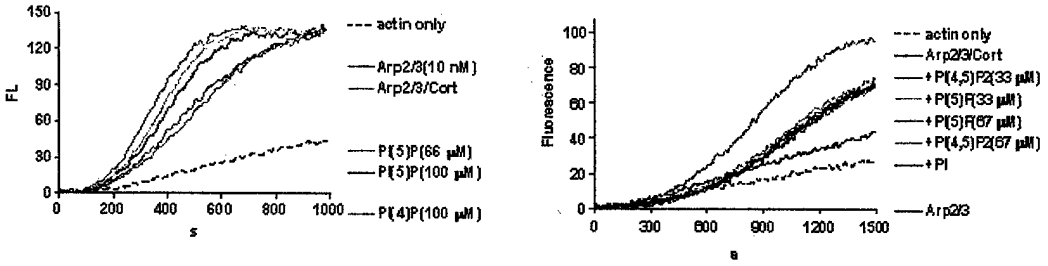

Figure 1. The effect of phosphatidylinositol 5-phosphate (PI(5)P, phosphosphatidylinositol 4-phosphoate (PI(4)P and phosphatidylinositol 4,5-biophosphates (PI(4,5)P2 on cortactin/Arp2/3 mediate actin assembly

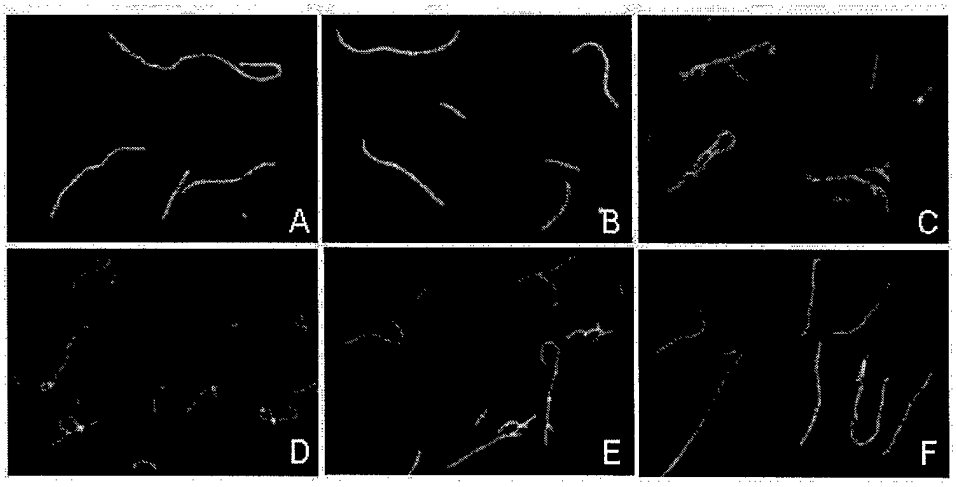

Figure 2. Effect of PIPs on actin branching induced by Arp2/3 complex and cortactin. (A) Actin only, (B) Arp2/3 only, (C) Arp2/3/Cort, (D) Arp2/3/Cort+PI(5)P (67 nM), (E) Arp2/3/Cort+PI(5)P (100 nM), (F) Arp2/3/Cort+PI(4)P (67 nM)

Key research accomplishments

1. Established the method to prepare liposomes and analyze the activity of phospholipids in actin assembly.

2. Established an effective RNAi-based method to knock down the function of cortactin in MDA-MB-231 breast cancer cells.

3. Determined a key biochemical reaction by which cortactin promotes actin branching

Reportable outcomes

1.Uruno T, Zhang P, Liu J, Jian-Jiang H, **Zhan X**. Hemaptopietic lineage cell specific protein 1 (HS1) promotes the Arp2/3 complex-mediated actin polymerization. Biochem J 2003; 371, 485-493.

2.Uruno T., Liu, J., Li, Y., Smith, N., **Zhan X**. Sequential interaction of Arp2/3 complex with N-WASP and cortactin during branched actin filament network formation. J. Biol. Chem. 2003; 278, 26086-93

3.Van Rossum A., Graaf, JHD; Schuuring-Scholites, E.; Kluin PM.; Fan Y.; **Zhan X**.; Moolenaar WH.; Schuuring Ed. Alternative splicing of the actin-binding domain of human cortactin affects cell migration. J. Biol. Chem. 2003 (in press)

4.Li Y., Uruno T., Haudenschild, C., Dudek, SM, Garcia JGN, **Zhan X**. Interaction of cortactin and Arp2/3 complex is required for sphingosine-1-phosphate induced endothelial cell morphogenesis and migration. Molecular Biological Cell (in revision)

5.Di Ciano C, Nie Z, Szaszi K, Lewis A, Uruno T, **Zhan X**, Rotstein OD, Mak A, Kapus A. Osmotic stress-induced remodeling of the cortical cytoskeleton Am J Physiol Cell Physiol 2002; 283: 850-865

Conclusions

1. Different types of phospholipids exhibit different specific activity on cortactin. PI(4)P inhibits cortactin while PI(5)P enhances the activity of cortactin.

2. Cortactin is essential for the formation of invadopodia of breast cancer cells.

Biochem. J. (2003) 371, 485–493 (Printed in Great Britain)

Haematopoietic lineage cell-specific protein 1 (HS1) promotes actin-related protein (Arp) 2/3 complex-mediated actin polymerization

Takehito URUNO*, Peijun ZHANG*†, Jiali LIU*, Jian-Jiang HAO* and Xi ZHAN*‡[1]

*Department of Experimental Pathology, Jerome H. Holland Laboratory for the Biomedical Sciences, American Red Cross, 15601 Crabbs Branch Way, Rockville, MD 20855, U.S.A., †Institute of Oceanology, Chinese Academy of Sciences, Qingdao 266071, People's Republic of China, and ‡Department of Cell Biology and Anatomy, The George Washington University, Washington, DC 20001, U.S.A.

HS1 (haematopoietic lineage cell-specific gene protein 1), a prominent substrate of intracellular protein tyrosine kinases in haematopoietic cells, is implicated in the immune response to extracellular stimuli and in cell differentiation induced by cytokines. Although HS1 contains a 37-amino acid tandem repeat motif and a C-terminal Src homology 3 domain and is closely related to the cortical-actin-associated protein cortactin, it lacks the fourth repeat that has been shown to be essential for cortactin binding to filamentous actin (F-actin). In this study, we examined the possible role of HS1 in the regulation of the actin cytoskeleton. Immunofluorescent staining demonstrated that HS1 co-localizes in the cytoplasm of cells with actin-related protein (Arp) 2/3 complex, the primary component of the cellular machinery responsible for *de novo* actin assembly. Furthermore, recombinant HS1 binds directly to Arp2/3 complex with an equilibrium dissociation constant (K_d) of 880 nM. Although HS1 is a modest F-actin-binding protein with a K_d of 400 nM, it increases the rate of the actin assembly mediated by Arp2/3 complex, and promotes the formation of branched actin filaments induced by Arp2/3 complex and a constitutively activated peptide of N-WASP (neural Wiskott–Aldrich syndrome protein). Our data suggest that HS1, like cortactin, plays an important role in the modulation of actin assembly.

Key words: actin cytoskeleton haematopoietic cell, cortactin, tyrosine kinase, Wiskott–Aldrich syndrome protein (WASP).

INTRODUCTION

The actin cytoskeleton plays a fundamental role in the function of haematopoietic cells, including antigen-mediated activation of lymphatic receptors [1,2], platelet activation [3] and adhesion of leucocytes to vascular cells [4]. While signalling cascades from extracellular stimuli often lead to changes in the dynamics of the actin cytoskeleton, the molecular mechanism by which the actin cytoskeleton is regulated in haematopoietic cells had not been known until the recent discovery of Wiskott–Aldrich syndrome protein (WASP) and actin-related protein (Arp) 2/3 complex [5–8]. Arp2/3 complex contains two actin-related subunits, Arp2 and Arp3, and five other unique polypeptides [9]. Under physiological conditions, Arp2/3 complex binds to the side of an actin filament, serves as the nucleation site for the assembly of monomeric actin, and generates branched actin filaments, which compose a characteristic actin network, filling up the areas within cell leading edges including lamellipodia and membrane ruffles. However, the stimulation of the nucleation activity of Arp2/3 complex requires the function of WASP or its related proteins, which interact with and activate Arp2/3 complex upon binding to membrane-associated small GTPases such as Cdc42 [7,10,11]. Whereas WASP and small GTPases constitute an important pathway from extracellular signals to the actin network, other signalling molecules such as the non-receptor protein tyrosine kinase Src and its related proteins are also known to be implicated in the modulation of the actin cytoskeleton [12]. However, the key substrate(s) of the Src family kinases responsible for cytoskeletal reorganization in haematopoietic cells remain unknown.

HS1 (haematopoietic lineage cell-specific gene protein 1) was originally isolated as a putative transcription factor exclusively expressed in haematopoietic cells [13]. However, subsequent studies indicate that HS1 is mainly a cytoplasmic protein and is often phosphorylated at tyrosine residues upon activation of membrane receptors including B-cell antigen receptor [14,15], CD3 T-cell receptors [16] and Fc ϵRI of mast cells [17]. Increased tyrosine phosphorylation of HS1 is also concomitant with the activation of one or several intracellular protein tyrosine kinases such as Lck, Syk, Lyn, Fgr and TPK-IIB [14,18–21]. Direct association of HS1 with Lyn and Lck has been described in T-cells and during the differentiation of erythroid cells mediated by erythropoietin [15,19,22,23]. The physiological function of HS1 is further illustrated by the study of HS1-knockout mice, which displayed a defect in antigen-induced proliferation and depletion of lymphocytes [24]. There is also evidence showing that HS1 is implicated in the apoptotic response to the activation of antigen receptors on lymphocytes, and lymphatic cells with low levels of HS1 expression have acquired a resistance to apoptosis [25]. Consistent with its role in apoptosis, HS1 is able to bind via its Src homology 3 (SH3) domain to HAX, a Bcl-2-like protein [26].

HS1 contains 3.5 37-amino acid tandem repeats and also an SH3 domain at the C-terminus. This structure is closely related to that of cortactin, an intracellular protein expressed primarily in adherent cells [27,28]. The amino acid sequences of the N-terminus, the repeat motif and the SH3 domain of HS1 share

Abbreviations used: Arp, actin-related protein; DTT, dithiothreitol; F-actin, filamentous actin; G-actin, globular actin; GFP, green fluorescent protein; GST, glutathione S-transferase; HS1, haematopoietic lineage cell-specific gene protein 1; N-WASP, neural WASP; SH3, Src homology 3; VCA, verprolin–cofilin–acidic motif; WASP, Wiskott–Aldrich syndrome protein.

[1] To whom correspondence should be addressed, at the Department of Experimental Pathology, Jerome H. Holland Laboratory for the Biomedical Sciences (e-mail zhanx@usa.redcross.org).

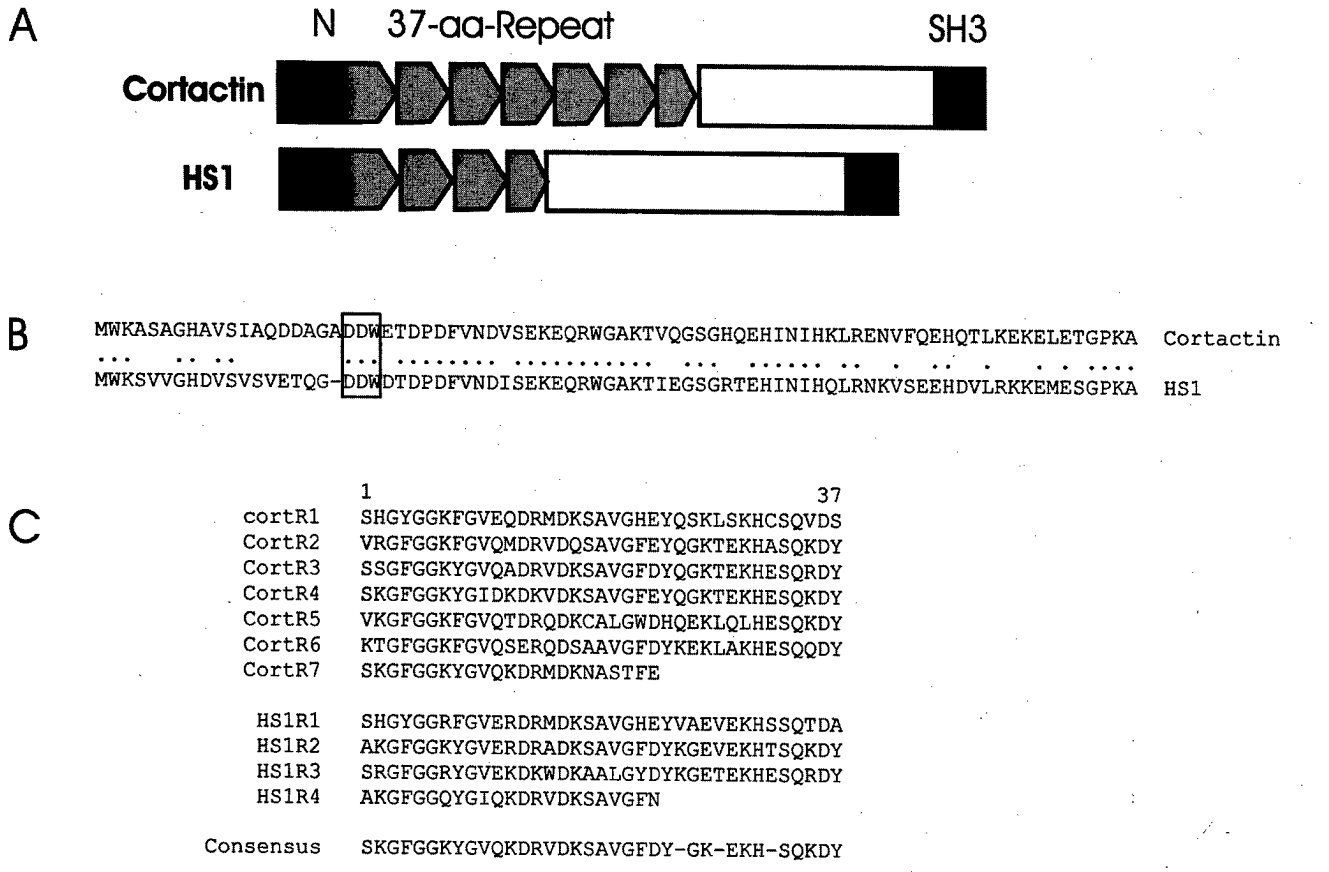

Figure 1 Structural comparison of cortactin and HS1

(**A**) Schematic presentation of cortactin and HS1. The N-terminal region, the 37-amino acid repeat and SH3 domain are indicated with different degrees of shading. (**B**) Alignment of the N-terminal sequence of human cortactin and human HS1. Identical amino acids are indicated by dots between them. The DDW motif, which is essential for cortactin binding to Arp2/3 complex, is boxed. (**C**) Alignment of the repeats of human cortactin and human HS1. Each repeat is denoted on the left by CortR or HS1R followed by a number corresponding to its position in the sequence. The consensus sequence, as defined using residues with an occurrence of more than 50%, is also shown.

identities of over 65% with those of cortactin (Figure 1), whereas the region between the repeat and the SH3 domain, which contains a putative α-helix, two or three phosphotyrosyl residues and a proline-rich region, is less conserved. Like HS1, cortactin is also known to be implicated in growth-factor signal transduction and acts as a primary substrate of Src-related kinases [29,30]. Recent studies demonstrated further that cortactin is an Arp2/3-complex stimulator and modulates the dynamics of the actin cytoskeleton [31,32]. *In vivo*, cortactin is tightly associated with the cortical actin and co-localizes with the Arp2/3 complex within punctated structures and the cell leading edge. *In vitro*, cortactin binds directly to the Arp2/3 complex, enhances the actin nucleation activity of the Arp2/3 complex and promotes the formation of actin branches during actin polymerization [31,32].

The distinguishing structural feature of HS1 is that it contains only 3.5 repeat units, which is in contrast to the 5.5 or 6.5 repeat units frequently found in cortactin isoforms. Whereas the repeat domain of cortactin is known to be responsible for filamentous actin (F-actin) binding, it requires at least 4 repeat units for F-actin binding [29,31]. In particular, the cortactin fourth repeat has been implicated in a direct interaction with F-actin [33], which is apparently missing in HS1. Therefore, the role of HS1 in the modulation of the actin cytoskeleton has not yet been established. In fact, a previous study was unable to determine a significant level of HS1 associated with F-actin [34], although its interaction with the actin cytoskeleton was assumed [35]. In the present study, we show that HS1 is able to bind to F-actin with modest affinity compared with cortactin. Furthermore, HS1 is able to interact directly with Arp2/3 complex and activate the Arp2/3-complex-mediated actin nucleation and branching in a manner similar to cortactin. Thus our study indicates that modulating actin assembly is a common function with both cortactin and HS1.

MATERIALS AND METHODS

Antibodies

Monoclonal antibody against green fluorescent protein (GFP) was purchased from Molecular Probes. Polyclonal antibodies against a human Arp3 peptide and recombinant human HS1 tagged with glutathione S-transferase (GST) were prepared as described previously [31,34]. All polyclonal antibodies were purified by Protein A–Sepharose 4 Fast Flow (Amersham Biosciences) affinity chromatography as described previously [30].

Plasmid construction

Plasmid pGST-HS1 was constructed as described previously [34]. A His-tagged HS1 plasmid (pQEHS1) was constructed by

inserting a PCR-generated human HS1 DNA based on pGST-HS1 into the *Bam*HI and *Sal*I sites of pQE-30 (Qiagen). The pQEHS1 plasmid was selected in XL1-Blue bacterial cells (Stratagene). The nucleotide sequence of the coding region was confirmed by DNA sequencing. Plasmid pHS1-GFP was prepared with the aid of PCR using pGST-HS1 as the template and the primers 5′-AGCTCAGAATTCATGTGGAAGTCTGTAGTGGGC-3′ and 5′-AGCTCAGTCGACCACTCCAGAAGCTTGACATA-3′. The resulting DNA fragment was inserted into *Eco*RI/*Sal*I sites of pEGFP1-N1 (Clontech).

Preparation of GST-HS1 and His-HS1 proteins

GST-HS1 was prepared as described previously [34]. To purify His-HS1 protein, XL1-Blue cells harbouring the pQEHS1 plasmid were grown at 37 °C to a density of $D_{600} = 0.6$, and expression was induced by adding 0.5 mM isopropyl β-D-thiogalactoside ('IPTG') followed by incubation at 34 °C with constant shaking at 250 rev./min for 4 h. The bacteria were harvested by centrifugation at 4000 *g* for 20 min and resuspended in lysis buffer (50 mM NaH_2PO_4, pH 8.0, 300 mM NaCl and 10 mM imidazole) at a ratio of 4 ml/g (wet weight). Lysozyme was added to a final concentration of 1 mg/ml and the lysate was subsequently incubated on ice for 30 min. The lysate was further subjected to sonication with an ultrasonic microprobe using a setting of six 10 s bursts at 200–300 W with a 10 s cooling period between each burst. After sonication, Triton X-100 was added to a final concentration of 1 % and the lysate was incubated on ice for 20 min. The lysate was then centrifuged at 10000 *g* for 20 min. The supernatant was mixed with 50 % (v/v) slurry of Ni^{2+}-nitrilotriacetic acid ('Ni-NTA') resin and incubated for 1 h at 4 °C in a rotator at 20 rev./min. After washing with lysis buffer containing 20 mM imidazole, His-HS1 was eluted with the same buffer containing 250 mM imidazole. The eluate was loaded on to a Mono-Q column on a Waters 600 pump in 50 mM Tris/HCl, pH 7.5, containing 1 mM dithiothreitol (DTT) and 1 mM EGTA, and eluted against a KCl gradient from 0 to 1 M in the same buffer at 1 ml/min. The major peak was collected and concentrated with Centricon-10 (Millipore). The concentration of purified protein was determined by the Bradford method using BSA as a standard. The purified His-HS1 protein was divided into small aliquots and stored at −80 °C.

Purification of Arp2/3 complex

Arp2/3 complex was purified from bovine brain extracts by a two-step procedure as described in [7] with a modification. Briefly, frozen bovine brain (100 g) was sliced with blades and homogenized with a dispersion device (Polytron PT 2100; Kinematica AG) on ice in 100 ml of buffer Q (20 mM Tris/HCl, pH 8.0, 100 mM NaCl, 5 mM $MgCl_2$, 5 mM EGTA and 1 mM DTT) supplemented with 50 μg/ml PMSF, 5 μg/ml leupeptin and 1 μg/ml aprotinin. The homogenized sample was then clarified by centrifugation at 125000 *g* for 90 min at 4 °C, and the supernatant was subjected to chromatography in a 100 ml Q Sepharose column equilibrated with buffer Q. The flow-through containing Arp2/3 complex was collected, supplemented with 0.1 mM ATP and fractionated on a GST-verprolin–cofilin–acidic motif (VCA) glutathione–Sepharose column equilibrated with buffer B (50 mM Tris/HCl, pH 7.5, 25 mM KCl, 1 mM $MgCl_2$, 0.5 mM EDTA, 1 mM DTT and 0.1 mM ATP). After washing with 0.2 M KCl in buffer B, the Arp2/3 complex was eluted with buffer B containing 0.2 M $MgCl_2$. The protein was then dialysed against buffer Q and further subjected to additional chromatography using Q Sepharose to remove residues of GST-VCA. The protein in the flow-through fraction of the second Q Sepharose fractionation was concentrated by a Centricon-30 (Millipore), and the buffer was changed to Ca^{2+}-free 1 × polymerization buffer (50 mM KCl, 2 mM $MgCl_2$, 1 mM EGTA, 0.25 mM ATP, 10 mM Tris/HCl, pH 7.3, 3 mM NaN_3 and 0.5 mM DTT). Protein concentration was determined by Bradford method using BSA as the standard.

Analysis of the interaction between HS1 and Arp2/3 complex

Purified GST-HS1 (5 or 10 μg) immobilized on glutathione–Sepharose (Amersham Biosciences) was mixed with 10 pmol of Arp2/3 complex in 500 μl of buffer A (50 mM Tris/HCl, pH 8.0, 150 mM NaCl and 1 % Triton X-100), and incubated at 4 °C on a rotating wheel for 90 min. After brief centrifugation, the beads were washed twice with buffer A and dissolved in 20 μl of 2 × SDS loading buffer. The amount of Arp2/3 complex in the beads was quantified by immunoblotting using a polyclonal anti-Arp3 antibody after separation by SDS/PAGE.

To analyse the affinity of HS1 for Arp2/3 complex, purified Arp2/3 complex (4 nM) was incubated with immobilized GST-HS1 at different concentrations for 90 min at 4 °C in binding buffer (50 mM Tris/HCl, pH 7.5, 1 mM EGTA, 0.1 mM $CaCl_2$, 0.5 mM DTT, 3 mM NaN_3, 50 mM KCl, 2 mM $MgCl_2$, 0.2 mM ATP, 0.2 mg/ml BSA and 0.1 % Tween-20). After incubation, samples were centrifuged at 800 *g* in a microcentrifuge for 10 s and the supernatants were then fractionated by SDS/PAGE (12 %, v/v, gels) and immunoblotted with polyclonal anti-Arp3 antibody. The proteins that were reactive to Arp3 antibody were detected by enhanced chemiluminescence (ECL) with an optimal exposure time that yielded a near-linear detection range based on purified Arp2/3 complex at three known concentrations that were loaded on the same gel. The densities of Arp3 bands shown on the blot, which represented unbound Arp3, were scanned and quantified with Scion Image software. The amounts of Arp3 depletion by different concentrations of GST-HS1 were used to fit a single rectangular hyperbola using GraphPad Prism 3, and the K_d value was calculated on the basis of $V = V_{max}C/(K_d + C)$, where V is the depletion of Arp3 proteins in the supernatant and C is the concentration of unbound HS1. The same methodology was also used in the measurement of the affinity for GST-VCA and GST-cortactin.

Actin-polymerization assay

Polymerization of globular actin (G-actin; 10 % pyrene-labelled) was performed as described in [31] with a modification. Briefly, Ca^{2+}ATP–G-actin in G-buffer (5 mM Tris/HCl, pH 8.0, 0.2 mM $CaCl_2$, 0.5 mM DTT and 0.2 mM ATP) was converted into Mg^{2+}ATP–G-actin by mixing with 0.1 vol. of 10 × exchange buffer (2 mM EGTA/1 mM $MgCl_2$) at 20 °C for 2 min [36–38]. Actin polymerization was initiated by adding 60 μl of Mg^{2+}ATP–G-actin (10 μM) to 240 μl of 1.25 × polymerization buffer (62.5 mM KCl, 2.5 mM $MgCl_2$, 12.5 mM imidazole, pH 7.3, 1.25 mM EGTA, 0.125 mM $CaCl_2$, 0.625 mM DTT, 0.3125 mM ATP and 3.75 mM NaN_3) in the presence of Arp2/3 complex and His-HS1 at the concentrations indicated. Actin assembly was monitored by measuring the increase in pyrene fluorescence detected with an LS50B spectrophotometer (Perkin Elmer) with filters for excitation at 365 nm and emission at 407 nm.

F-actin branching assay

F-actin branching assay was based on a method that was described previously [39]. Briefly, polymerization of 2.0 μM monomeric actin was initiated by 30 nM His-HS1 in the presence

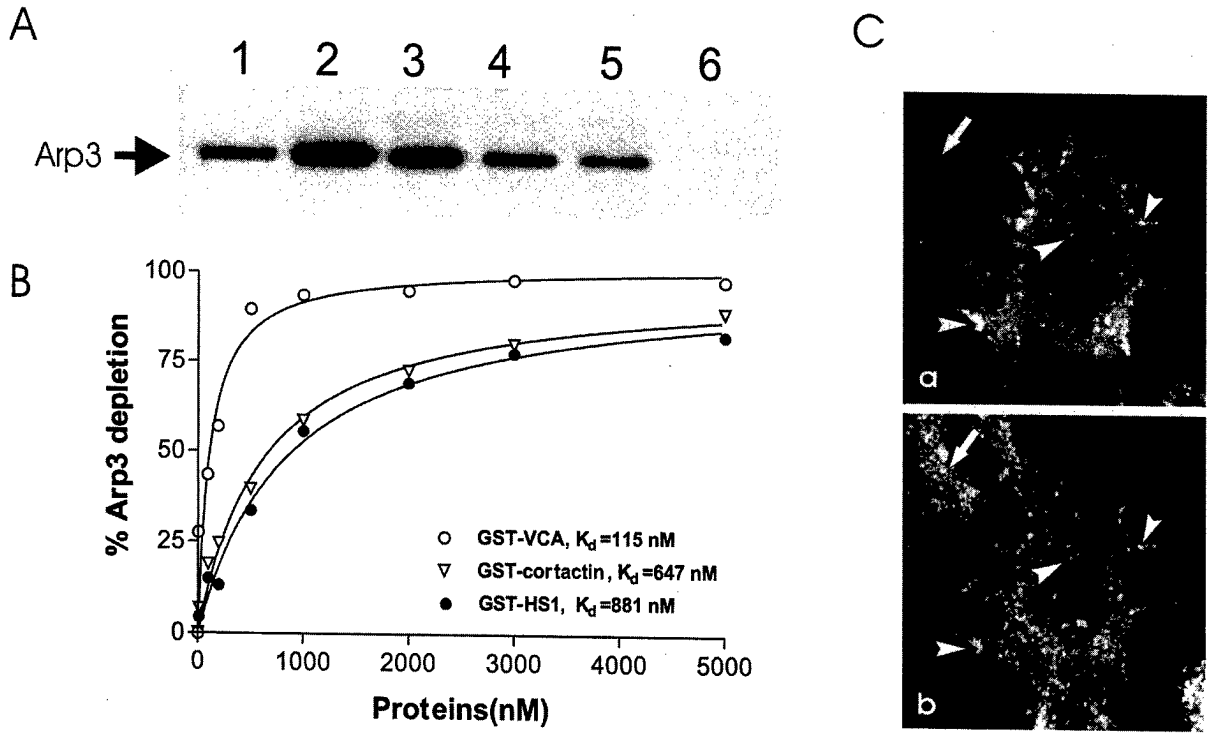

Figure 2 The interaction of HS1 and Arp2/3 complex

(**A**) Pull-down analysis of the interaction of HS1 with Arp2/3 complex. GST-VCA or GST-HS1 at various concentrations was mixed with 88 nM Arp2/3 complex as described in the Materials and methods section. After incubation for 90 min at 4 °C, GST-conjugated proteins were precipitated by glutathione beads. The presence of Arp2/3 complex in the pellet was analysed by immunoblotting with Arp3 antibody. Lane 1, 0.1 pmol of Arp2/3 complex; lane 2, 600 nM GST-VCA; lanes 3–5, GST-HS1 at 600, 300 and 150 nM, respectively; lane 6, GST, 300 nM. (**B**) Comparison of the affinity of GST-HS1, GST-cortactin and GST-VCA for Arp2/3 complex. Purified Arp2/3 complex (4.4 nM) was mixed with different amounts of immobilized GST-HS1, GST-cortactin or GST-VCA. After 90 min of incubation at 4 °C, samples were centrifuged at 800 ***g*** for 10 s. The presence of Arp3 in the supernatants was detected by immunoblot with anti-Arp3 antibody. Amounts of Arp3 were quantified by digital scanning and normalized to the percentage of depletion. The resulting data were used to fit a rectangular hyperbola, yielding apparent K_d values of 881, 647 and 115 nM for GST-HS1, GST-cortactin and GST-VCA, respectively. (**C**) Immunofluorescent staining of HS1-GFP and Arp2/3 complex within macrophage cells. Raw 264.7 macrophage cells were transiently transfected with pHS1-GFP. The transfected cells were fixed and double-stained with monoclonal anti-GFP antibody (panel **a**) and polyclonal anti-Arp3 antibody (panel **b**). The arrowheads indicate representative locations where HS1-GFP and Arp3 were apparently co-localized. A non-transfected cell, as shown in panels (**a**) and (**b**), is indicated by an arrow.

of 30 nM GST-VCA and 8 nM Arp2/3 complex. To visualize actin branches, a molar equivalent of rhodamine–phalloidin (Molecular Probes) was added to the reaction solution at given times after initiation. Samples were diluted 400-fold in fresh fluorescence buffer (100 mM KCl, 1 mM $MgCl_2$, 100 mM DTT, 10 mM imidazole, pH 7.3, 0.5% methylcellulose, 20 μg/ml catalase, 100 μg/ml glucose oxidase and 3 mg/ml glucose). Diluted samples (2.0 μl) were applied on to coverslips precoated with 0.1% nitrocellulose in *n*-amyl acetate. Actin filaments were examined by an Olympus IX-70 inverted microscope using a 100 × 1.35 NA objective lens. Images were captured with a digital camera controlled by the SPOT advance software. The digital images were processed with Adobe Photoshop to generate monochromatic images. Actin branches were quantified by measuring the density of branches (number of branch points/filament length) from five randomly selected images using Scion Image software.

F-actin binding assay

F-actin was prepared by incubating G-actin in polymerization buffer at room temperature for 4 h. To compare the F-actin binding ability of HS1 with cortactin, F-actin at different concentrations was mixed with 30 nM His-HS1 or His-cortactin followed by incubation for 30 min at room temperature. The concentration of F-actin was calculated by the subtraction of 0.1 μM from the concentration of G-actin. The reaction solution was centrifuged at 200000 ***g*** for 30 min to pellet the bound proteins. The unbound His-HS1 or His-cortactin proteins in the supernatant were fractionated by SDS/PAGE and detected by immunoblotting using antibodies against HS1 or cortactin.

Immunofluorescence analysis

Murine macrophage cell line Raw 264.7 was from the A.T.C.C. The cells were maintained in Dulbecco's modified Eagle's medium plus 10% fetal bovine serum. The cells at logarithmic phase were transfected with plasmids pHS1-GFP or pEGFP1-N1 with Superfect (Qiagen). After 24 h, the transfected cells were plated on fibronectin-coated glass coverslips in the growth medium. After an additional 12 h incubation, the cells were permeabilized by incubation for 20 s in 0.1 M Mes, pH 7.4, containing 0.2% Triton X-100, 1 mM $MgCl_2$, 1 mM EGTA and 4% poly(ethylene glycol) 6000. The permeabilized cells were subsequently fixed for 30 min in 3.7% paraformaldehyde in PBS followed by three washes with PBS. The cells were then incubated for 30 min in PBS containing 2% BSA followed by a 1 h incubation in the same buffer containing polyclonal anti-Arp3 antibody at a concentration of 50 μg/ml and monoclonal anti-GFP antibody at 10 μg/ml. After three washes with PBS, secondary antibodies (rhodamine-conjugated anti-rabbit IgG and fluorescein-conjugated anti-mouse IgG antibodies) were applied. After 1 h

incubation, cells were washed with PBS and mounted in Prolong antifade solution (Molecular Probes) on a glass slide. The samples were examined by confocal laser microscopy using a Bio-Rad Radiance 2100 laser scanning system equipped with a Nikon Eclipse E800 microscope.

RESULTS

HS1 interacts directly with Arp2/3 complex

The interaction between HS1 and Arp2/3 complex was first examined using a pull-down assay using GST-HS1 and purified bovine Arp2/3 complex. As shown in Figure 2(A), GST-HS1 at concentrations ranging from 150 to 600 nM (Figure 2A, lanes 3–5) was able to pull down readily 88 nM Arp2/3 complex as indicated by the presence of Arp3, a subunit of Arp2/3 complex, in the pellets, whereas GST alone (Figure 2A, lane 6) precipitated no detectable Arp3 as analysed by immunblot. Analysis of the Arp3 remaining in the supernatant after pull-down estimated a K_d of 881 nM for the binding of GST-HS1 to Arp2/3 complex. This K_d value is very similar to that of cortactin (K_d = 647 nM) but significantly greater than that of GST-VCA (K_d = 115 nM), a constitutively active peptide of human neural WASP (N-WASP; Figure 2B) [7]. The similar affinities of HS1 and cortactin

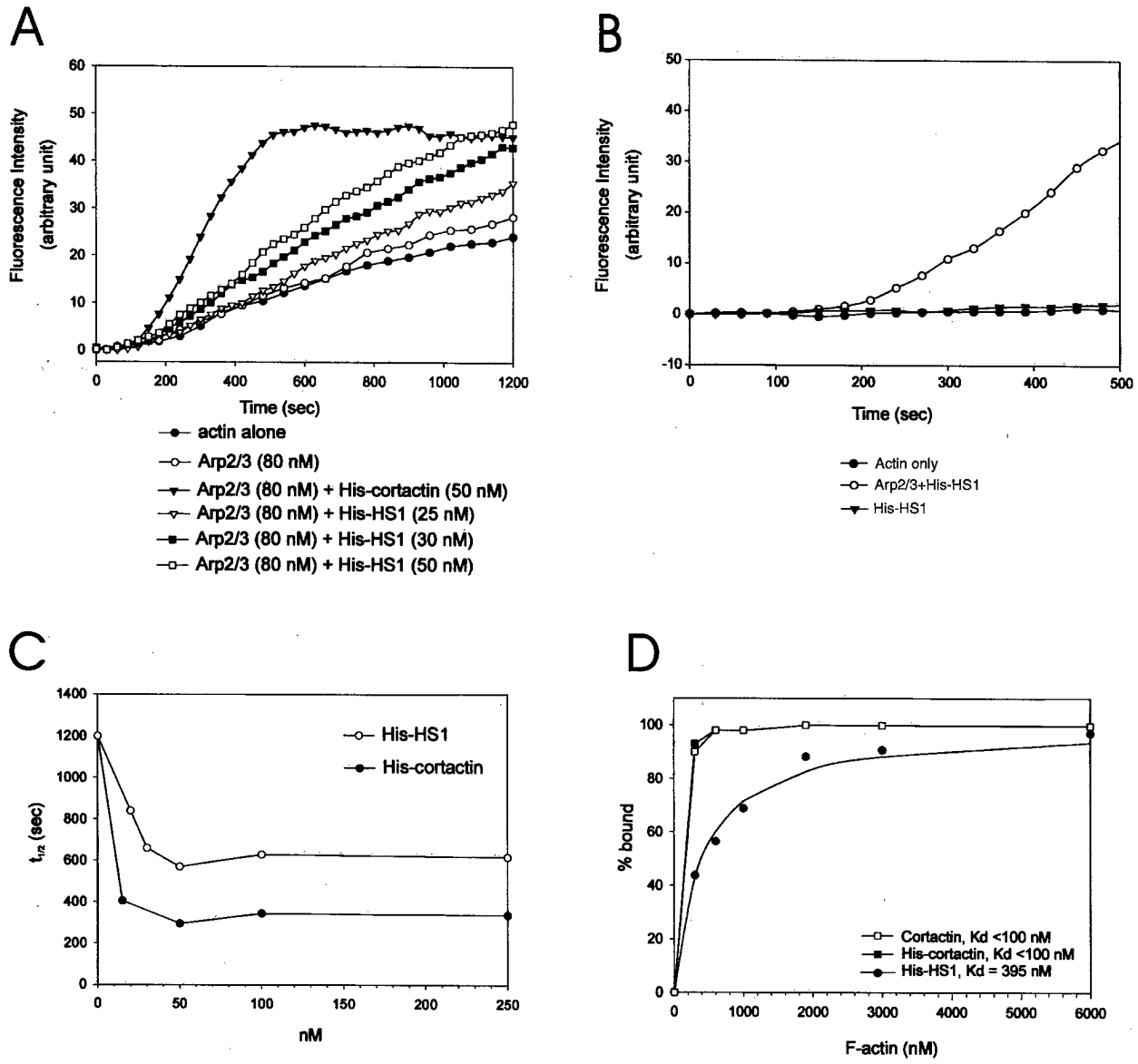

Figure 3 HS1 promotes actin polymerization nucleated by Arp2/3 complex

(**A**) Actin-polymerization analysis. Polymerization of 2 μM 10% pyrene-labelled G-actin was initiated with 80 nM Arp2/3 complex and His-HS1 at the indicated concentrations. For comparison, 50 nM His-cortactin was also analysed in parallel. (**B**) His-HS1 alone does not have actin-assembly-promoting activity. The conditions were the same as in (**A**) except that His-HS1 was used at 80 nM and Arp2/3 complex at 14 nM. (**C**) Comparison of the activities of His-HS1 and His-cortactin for actin polymerization based on the time required for achieving 50% of a maximal actin polymerization ($t_{1/2}$). (**D**) Comparison of the affinities of HS1 and cortactin for F-actin: 30 nM His-HS1, His-cortactin or tag-free cortactin was co-precipitated with F-actin at concentrations ranging from 0.3 to 6 μM. The K_d values were estimated as described in the Materials and methods section. The estimated K_d for His-HS1 was 395 nM and that for either His-cortactin or tag-free cortactin was less than 100 nM.

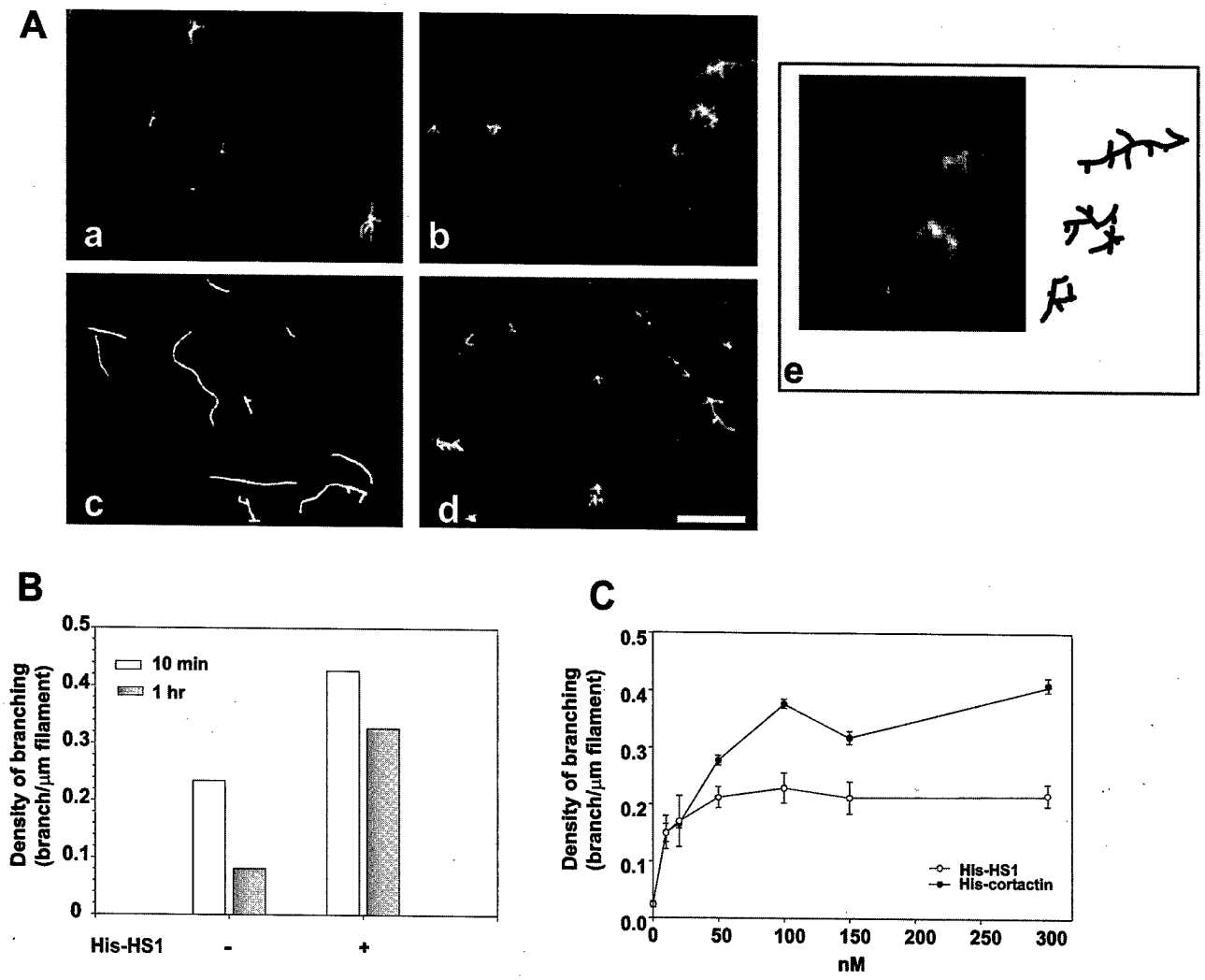

Figure 4 HS1 promotes the formation of stable F-actin branches

(**A**) Actin polymerization was initiated by 8 nM Arp2/3 complex and 30 nM GST-VCA in the absence (**a**, **c**) or presence (**b**, **d**) of 30 nM His-HS1. After 10 min (**a**, **b**) or 1 h (**c**, **d**), rhodamine–phalloidin at molar concentrations equivalent to monomer actin was added. The labelled actin filaments were examined under a fluorescent microscope. Scale bar (**d**), 5 μm. Panel (**e**), an enlarged image derived from (**b**) is shown on the left. On the right a sketch for the reconstruction of these branched actin complexes is presented. (**B**) Quantification of HS1-mediated actin branching. The branch density was calculated based on the ratio of the number of branching sites to the length of the filament in five randomly selected images from the same experiment as presented in (**A**). Each data point was calculated based on the measurement of actin filaments of more than 200 μm in length. (**C**) Comparison of the actin branching activity of His-HS1 with His-cortactin. Actin branching was initiated in the presence of 8 nM Arp2/3 complex, 30 nM GST-VCA, and His-HS1 or His-cortactin at the indicated concentrations. The density of actin branching at each concentration was calculated based on the average branching sites counted from 200 μm actin filaments.

for Arp2/3 complex is consistent with a conserved sequence of 63% identity in their N-termini, which includes the DDW motif that has been demonstrated to be critical for cortactin binding to Arp2/3 complex (Figure 1B) [31].

The interaction of HS1 and Arp2/3 complex was further examined by analysing murine Raw 264.7 macrophage cells overexpressing a form of human HS1 tagged with GFP at its C-terminus (HS1-GFP). The cellular distributions of HS1-GFP and endogenous Arp2/3 complex were analysed by immunofluorescence staining with a monoclonal anti-GFP antibody and polyclonal anti-Arp3 antibody, respectively. As shown in Figure 2(C), both HS1-GFP and Arp3 are found in punctate-like structures enriched within the cell periphery and the cytoplasm. In many punctates, co-localization of HS1-GFP and Arp3 is evident. The specificity of the staining was verified by negative GFP staining of a non-transfected cell as indicated by an arrow (Figure 2C, panels a and b) and cells expressing GFP only (results not shown).

HS1 promotes actin assembly nucleated by Arp2/3 complex

Arp2/3 complex is a primary cellular factor involved in actin nucleation, a rate-limiting step for *de novo* synthesis of actin filaments [9]. Therefore, we determined whether binding of HS1 to Arp2/3 complex had any influence on actin assembly. The effect of HS1 on the nucleation activity of Arp2/3 complex was evaluated by measuring the polymerization of pyrene-labelled G-actin. The rate of actin polymerization was apparently enhanced in the presence of both His-HS1 and Arp2/3 complex (Figure 3A). Half-maximal actin polymerization was reached within 600 s in the presence of 50 nM His-HS1 and 80 nM Arp2/3. However, the rate of His-HS1-stimulated actin growth appeared

to be lower than that of His-cortactin, which was able to induce half-maximal stimulation in approx. 300 s under the same conditions (Figure 3A). The apparent activity of His-HS1 in actin assembly was probably due to its interaction with Arp2/3 complex because no significant increase in actin polymerization was detected in the presence of either Arp2/3 (Figure 3A) or His-HS1 alone (Figure 3B). The activities of HS1 and cortactin were also compared by their dose-dependent stimulation of half-maximal actin assembly ($t_{\frac{1}{2}}$; Figure 3C). Whereas His-cortactin has an apparent higher potency than His-HS1, both proteins showed 50% stimulation at a concentration near 25 nM and maximal stimulation at 50 nM. Thus, like cortactin, HS1 has apparently a high functional efficacy for Arp2/3 complex during actin polymerization although its binding affinity for Arp2/3 is low.

HS1 is a modest F-actin-binding protein

Cortactin is known as a potent F-actin-binding protein through its repeat domain, and its affinity for F-actin appears to be crucial for its stimulation of Arp2/3-mediated actin assembly [31]. The apparent activity of HS1 to stimulate Arp2/3 complex suggests that HS1 may be an F-actin-binding protein as well. However, HS1 has a short repeat domain (3.5 37-amino acid tandem repeats) and its ability to bind to F-actin has not yet been established. We examined the interaction of HS1 with F-actin by co-precipitation of His-HS1 and F-actin and quantified the interaction by plotting co-precipitated HS1 as a function of F-actin concentration (Figure 3D). This analysis estimated the K_d of His-HS1 for F-actin binding to be approx. 395 nM. In a parallel experiment, we also measured the affinity of His-cortactin for F-actin and estimated the K_d of His-cortactin at less than 100 nM (Figure 3D). A precise prediction of the K_d value for His-cortactin has not been achieved because the critical concentration of actin, approx. 100 nM under typical conditions for F-actin binding, put a limit on the lowest amount of F-actin available for measuring the affinity of His-cortactin. The possible effect of the His tag was ruled out by comparing His-cortactin and tag-free cortactin, both of which showed identical affinity for F-actin (Figure 3D) and actin assembly (results not shown). Thus, in spite of the lack of a fourth repeat, HS1 is an F-actin-binding protein but with modest affinity compared with cortactin.

HS1 promotes the formation of a branched actin network

A hallmark of the actin polymerization initiated by Arp2/3 complex is the formation of characteristic branched actin network, an activity that can be significantly enhanced by cortactin [32]. To examine whether HS1 has a similar branching activity as cortactin, actin polymerization was initiated by adding His-HS1, Arp2/3 complex and GST-VCA. GST-VCA was included in this study to fully activate the Arp2/3 complex and facilitate the measurement of the activity of HS1 for actin branching. After either 10 min or 1 h of initiation, actin was labelled with rhodamine–phalloidin and examined by fluorescence microscopy. Although many branched actin filaments in the presence of Arp2/3 complex and GST-VCA were readily detected at an early time (10 min; Figure 4A, panel a), longer and less-branched actin filaments became dominant after 1 h incubation (Figure 4A, panel c), presumably due to a debranching process followed by an annealing reaction [39]. Quantitative analysis based on the branch density also indicated that about two-thirds of the actin filaments formed without His-HS1 had undergone the debranching process after 1 h (Figure 4B). In contrast, the presence of His-HS1 yielded short and highly branched actin filaments with a density 1.8-fold higher than that formed in the absence of His-HS1 at 10 min and 4-fold higher at 1 h (Figure 4B).

The branching activity of His-HS1 was also compared with that of His-cortactin at different concentrations after 1 h of actin assembly. While the maximal actin branch density induced by His-HS1 appeared to be lower than that of His-cortactin by nearly 50%, both proteins were able to show a half-maximal stimulation near 25 nM and reach to a plateau at 100 nM (Figure 4C).

DISCUSSION

The data presented here demonstrate for the first time that HS1, a prominent substrate of intracellular protein tyrosine kinases in haematopoietic cells, may play a role in actin polymerization by its direct association with Arp2/3 complex, the primary component of the cellular machinery for actin assembly. Recombinant HS1 is able to bind to the Arp2/3 complex, and promote Arp2/3-mediated actin assembly and actin branching, the activity that is also observed with cortactin, the only protein in mammalian cells that shares significant sequence identity with HS1. However, the *in vivo* function of HS1 and cortactin may not be necessarily redundant because each of them shows a very distinct expression pattern. While HS1 is exclusively expressed in haematopoietic cells, cortactin is more frequently found in adherent types of cell. In addition, HS1 displays a relatively lower activity for the stimulation of actin nucleation and actin branching compared with cortactin. Such modest activity of HS1 may have a physiological function for haematopoietic cells, which have distinct morphology adapted to their circulation in blood vessels and interaction with vascular cells. Indeed, expression of cortactin in bone marrow is very restricted within limited types of cell, such as megakaryocytes and platelets, which have a characteristically large volume of cytoplasm and are ready to challenge stimuli for shape changes [28]. It is noteworthy that the WASP family, which currently includes WASP, N-WASP, WAVE1, WAVE2 and WAVE3, also shows a tissue-specific expression pattern for each of its members [9,40]. While WASP is exclusively expressed in haematopoietic cells, N-WASP is mostly found in a variety of adherent cells, particularly in the brain. In addition, each WASP member activates Arp2/3-dependent actin nucleation with differential efficiencies, with the strongest activity found with N-WASP [41,42]. Thus it seems that haematopoietic cells encompass a unique actin-polymerization system that involves HS1, WASP and the Arp2/3 complex. Characterization of the actin network assembled by these molecules may eventually illustrate a unique cytoskeleton more suitable for haematopoietic cells that circulate in the blood.

The apparent affinity of HS1 for Arp2/3 complex is significantly lower than that of GST-VCA, as analysed in the absence of actin. Interestingly, HS1 is able to induce half-maximal stimulation of Arp2/3-dependent actin polymerization and actin branching at a concentration near 25 nM (Figures 3C and 4C). However, the affinity of HS1 for Arp2/3, as determined by direct binding assay, was near 900 nM (Figure 2B). This apparent discrepancy between functional and binding affinity is also observed with cortactin (Figure 2B; see also [31]). One plausible explanation is that HS1 may acquire a higher affinity for Arp2/3 complex upon actin assembly. Indeed, a dramatic change in the configuration of Arp2/3 complex induced by WASP-related peptides has been postulated based on structural studies [43,44]. Such structural changes may influence the interaction between HS1 and Arp2/3 complex. Supporting this possibility is the observation that activated Arp2/3 complex is integrated with newly assembled F-actin at branched points, where cortactin and

WASP are apparently involved [31,32,45]. Alternatively, F-actin, especially newly assembled actin filaments, could also play a role in the regulation of the interaction between HS1 and Arp2/3 complex. Distinguishing these possibilities will require further delineation of the mechanism for actin polymerization and illustration of the structure of branched actin.

In addition to binding to Arp2/3 complex, HS1 shows a significant affinity for F-actin with an estimated K_d of 400 nM. Under the same conditions, we measured the K_d for cortactin to be less than 100 nM, which is slightly less than that estimated in previous studies [29,31]. This apparent discrepancy might be due to the improved methodology used in the current study, in which a low concentration (30 nM) of His-cortactin and freshly prepared F-actin were used. It has been reported that the repeat domain of cortactin is responsible for F-actin binding [29]. Particularly, the fourth repeat may participate in a direct interaction with F-actin because a series of truncated mutants lacking this repeat failed to show any F-actin binding activity [33]. However, HS1 contains only 3.5 repeats and lacks the fourth repeat found in cortactin. Thus binding of the cortactin family to F-actin seems not to be exclusively dependent on the existence of a particular repeat. It is more likely that F-actin binding requires a correct configuration of the repeat domain as a whole, which may be determined by both the number of repeats and their positions relative to F-actin at branching sites. Indeed, the sequence of the HS1/cortactin repeat unit is extremely conserved (Figure 1C). It is also possible that sequence elements other than the repeat domain of HS1 may also contribute to its F-actin binding activity. It is worth noting that the sequence that lies between the repeat and the SH3 domain of HS1 is much less conserved and shares only 25% identity with that of cortactin. This may reflect a different mechanism for the regulation of each protein *in vivo* and may impose different restrictions on their overall configurations as well.

We acknowledge Dr Christian Haudenschild for help with the confocal microscopy, Dr Jeff Winkles for critical reading, Dr Li Zhang for help with Raw 264.7 cell culture assistance and Ms Nicole Smith for technical assistance. This study was supported by National Institutes of Health RO1 HL 52753-09, Department of Defense grant DAMD17-01-1-0125 and American Heart Association Established Investigator grant 0040135N (to X.Z.).

REFERENCES

1 Acuto, O. and Cantrell, D. (2000) T cell activation and the cytoskeleton. Annu. Rev. Immunol. **18**, 165–184
2 Westerberg, L., Greicius, G., Snapper, S. B., Aspenstrom, P. and Severinson, E. (2001) Cdc42, Rac1, and the Wiskott-Aldrich syndrome protein are involved in the cytoskeletal regulation of B lymphocytes. Blood **98**, 1086–1094
3 Gallego, M. D., Santamaria, M., Pena, J. and Molina, I. J. (1997) Defective actin reorganization and polymerization of Wiskott-Aldrich T cells in response to CD3-mediated stimulation. Blood **90**, 3089–3097
4 Wojciak-Stothard, B., Williams, L. and Ridley, A. J. (1999) Monocyte adhesion and spreading on human endothelial cells is dependent on Rho-regulated receptor clustering. J. Cell Biol. **145**, 1293–1307
5 Machesky, L. M. and Insall, R. H. (1998) Scar1 and the related Wiskott-Aldrich syndrome protein, WASP, regulate the actin cytoskeleton through the Arp2/3 complex. Curr. Biol. **8**, 1347–1356
6 Yarar, D., To, W., Abo, A. and Welch, M. D. (1999) The Wiskott-Aldrich syndrome protein directs actin-based motility by stimulating actin nucleation with the Arp2/3 complex. Curr. Biol. **9**, 555–558
7 Egile, C., Loisel, T. P., Laurent, V., Li, R., Pantaloni, D., Sansonetti, P. J. and Carlier, M. F. (1999) Activation of the CDC42 effector N-WASP by the *Shigella flexneri* IcsA protein promotes actin nucleation by Arp2/3 complex and bacterial actin-based motility. J. Cell Biol. **146**, 1319–1332
8 Winter, D., Lechler, T. and Li, R. (1999) Activation of the yeast Arp2/3 complex by Bee1p, a WASP-family protein. Curr. Biol. **9**, 501–504
9 Higgs, H. N. and Pollard, T. D. (2001) Regulation of actin filament network formation through Arp2/3 complex: activation by a diverse array of proteins. Annu. Rev. Biochem. **70**, 649–676
10 Miki, H., Sasaki, T., Takai, Y. and Takenawa, T. (1998) Induction of filopodium formation by a WASP-related actin-depolymerizing protein N-WASP. Nature (London) **391**, 93–96
11 Rohatgi, R., Ma, L., Miki, H., Lopez, M., Kirchhausen, T., Takenawa, T. and Kirschner, M. W. (1999) The interaction between N-WASP and the Arp2/3 complex links Cdc42-dependent signals to actin assembly. Cell **97**, 221–231
12 Kellie, S., Horvath, A. R. and Elmore, M. A. (1991) Cytoskeletal targets for oncogenic tyrosine kinases. J. Cell Sci. **99**, 207–211
13 Kitamura, D., Kaneko, H., Miyagoe, Y., Ariyasu, T. and Watanabe, T. (1989) Isolation and characterization of a novel human gene expressed specifically in the cells of hematopoietic lineage. Nucleic Acids Res. **17**, 9367–9379
14 Yamanashi, Y., Okada, M., Semba, T., Yamori, T., Umemori, H., Tsunasawa, S., Toyoshima, K., Kitamura, D., Watanabe, T. and Yamamoto, T. (1993) Identification of HS1 protein as a major substrate of protein-tyrosine kinase(s) upon B-cell antigen receptor-mediated signaling. Proc. Natl. Acad. Sci. U.S.A. **90**, 3631–3635
15 Takemoto, Y., Furuta, M., Li, X. K., Strong-Sparks, W. J. and Hashimoto, Y. (1995) LckBP1, a proline-rich protein expressed in haematopoietic lineage cells, directly associates with the SH3 domain of protein tyrosine kinase p56lck. EMBO J. **14**, 3403–3414
16 Hutchcroft, J. E., Slavik, J. M., Lin, H., Watanabe, T. and Bierer, B. E. (1998) Uncoupling activation-dependent HS1 phosphorylation from nuclear factor of activated T cells transcriptional activation in Jurkat T cells: differential signaling through CD3 and the costimulatory receptors CD2 and CD28. J. Immunol. **161**, 4506–4512
17 Suzuki, H., Takei, M., Yanagida, M., Nakahata, T., Kawakami, T. and Fukamachi, H. (1997) Early and late events in Fc epsilon RI signal transduction in human cultured mast cells. J. Immunol. **159**, 5881–5888
18 Yamamoto, T., Yamanashi, Y. and Toyoshima, K. (1993) Association of Src-family kinase Lyn with B-cell antigen receptor. Immunol. Rev. **132**, 187–206
19 Takemoto, Y., Sato, M., Furuta, M. and Hashimoto, Y. (1996) Distinct binding patterns of HS1 to the Src SH2 and SH3 domains reflect possible mechanisms of recruitment and activation of downstream molecules. Int. Immunol. **8**, 1699–1705
20 Brunati, A. M., Ruzzene, M., James, P., Guerra, B. and Pinna, L. A. (1995) Hierarchical phosphorylation of a 50-kDa protein by protein tyrosine kinases TPK-IIB and C-Fgr, and its identification as HS1 hematopoietic-lineage cell-specific protein. Eur. J. Biochem. **229**, 164–170
21 Ruzzene, M., Brunati, A. M., Marin, O., Donella-Deana, A. and Pinna, L. A. (1996) SH2 domains mediate the sequential phosphorylation of HS1 protein by p72syk and Src-related protein tyrosine kinases. Biochemistry **35**, 5327–5332
22 Nagata, Y., Kiefer, F., Watanabe, T. and Todokoro, K. (1999) Activation of hematopoietic progenitor kinase-1 by erythropoietin. Blood **93**, 3347–3354
23 Ingley, E., Sarna, M. K., Beaumont, J. G., Tilbrook, P. A., Tsai, S., Takemoto, Y., Williams, J. H. and Klinken, S. P. (2000) HS1 interacts with Lyn and is critical for erythropoietin-induced differentiation of erythroid cells. J. Biol. Chem. **275**, 7887–7893
24 Taniuchi, I., Kitamura, D., Maekawa, Y., Fukuda, T., Kishi, H. and Watanabe, T. (1995) Antigen-receptor induced clonal expansion and deletion of lymphocytes are impaired in mice lacking HS1 protein, a substrate of the antigen-receptor-coupled tyrosine kinases. EMBO J. **14**, 3664–3678
25 Yamanashi, Y., Fukuda, T., Nishizumi, H., Inazu, T., Higashi, K., Kitamura, D., Ishida, T., Yamamura, H., Watanabe, T. and Yamamoto, T. (1997) Role of tyrosine phosphorylation of HS1 in B cell antigen receptor-mediated apoptosis. J. Exp. Med. **185**, 1387–1392
26 Suzuki, Y., Demoliere, C., Kitamura, D., Takeshita, H., Deuschle, U. and Watanabe, T. (1997) HAX-1, a novel intracellular protein, localized on mitochondria, directly associates with HS1, a substrate of Src family tyrosine kinases. J. Immunol. **158**, 2736–2744
27 Zhan, X., Hu, X., Hampton, B., Burgess, W. H., Friesel, R. and Maciag, T. (1993) Murine cortactin is phosphorylated in response to fibroblast growth factor-1 on tyrosine residues late in the G1 phase of the BALB/c 3T3 cell cycle. J. Biol. Chem. **268**, 24427–24431
28 Zhan, X., Haudenschild, C. C., Ni, Y., Smith, E. and Huang, C. (1997) Upregulation of cortactin expression during the maturation of megakaryocytes. Blood **89**, 457–464
29 Wu, H. and Parsons, J. T. (1993) Cortactin, an 80/85-kilodalton pp60src substrate, is a filamentous actin-binding protein enriched in the cell cortex. J. Cell Biol. **120**, 1417–1426
30 Zhan, X., Plourde, C., Hu, X., Friesel, R. and Maciag, T. (1994) Association of fibroblast growth factor receptor-1 with c-Src correlates with association between c-Src and cortactin. J. Biol. Chem. **269**, 20221–20224
31 Uruno, T., Liu, J., Zhang, P., Fan, Y., Egile, C., Li, R., Mueller, S. C. and Zhan, X. (2001) Activation of Arp2/3 complex-mediated actin polymerization by cortactin. Nat. Cell Biol. **3**, 259–266
32 Weaver, A. M., Karginov, A. V., Kinley, A. W., Weed, S. A., Li, Y., Parsons, J. T. and Cooper, J. A. (2001) Cortactin promotes and stabilizes Arp2/3-induced actin filament network formation. Curr. Biol. **11**, 370–374

33 Weed, S. A., Karginov, A. V., Schafer, D. A., Weaver, A. M., Kinley, A. W., Cooper, J. A. and Parsons, J. T. (2000) Cortactin localization to sites of actin assembly in lamellipodia requires interactions with F-actin and the Arp2/3 complex. J. Cell Biol. **151**, 29–40
34 He, H., Watanabe, T., Zhan, X., Huang, C., Schuuring, E., Fukami, K., Takenawa, T., Kumar, C. C., Simpson, R. J. and Maruta, H. (1998) Role of phosphatidylinositol 4,5-bisphosphate in Ras/Rac-induced disruption of the cortactin-actomyosin II complex and malignant transformation. Mol. Cell Biol. **18**, 3829–3837
35 Chen, Y. R., Kori, R., John, B. and Tan, T. H. (2001) Caspase-mediated cleavage of actin-binding and SH3-domain-containing proteins cortactin, HS1, and HIP-55 during apoptosis. Biochem. Biophys. Res. Commun. **288**, 981–989
36 Amann, K. J. and Pollard, T. D. (2001) The Arp2/3 complex nucleates actin filament branches from the sides of pre-existing filaments. Nat. Cell Biol. **3**, 306–310
37 Mullins, R. D. and Machesky, L. M. (2000) Actin assembly mediated by Arp2/3 complex and WASP family proteins. Methods Enzymol. **325**, 214–237
38 Pantaloni, D., Boujemaa, R., Didry, D., Gounon, P. and Carlier, M. F. (2000) The Arp2/3 complex branches filament barbed ends: functional antagonism with capping proteins. Nat. Cell Biol. **2**, 385–391
39 Blanchoin, L., Amann, K. J., Higgs, H. N., Marchand, J. B., Kaiser, D. A. and Pollard, T. D. (2000) Direct observation of dendritic actin filament networks nucleated by Arp2/3 complex and WASP/Scar proteins. Nature (London) **404**, 1007–1011
40 Suetsugu, S., Miki, H. and Takenawa, T. (2001) Identification of another actin-related protein (Arp) 2/3 complex binding site in neural Wiskott-Aldrich syndrome protein (N-WASP) that complements actin polymerization induced by the Arp2/3 complex activating (VCA) domain of N-WASP. J. Biol. Chem. **276**, 33175–33180
41 Yamaguchi, H., Miki, H., Suetsugu, S., Ma, L., Kirschner, M. W. and Takenawa, T. (2000) Two tandem verprolin homology domains are necessary for a strong activation of Arp2/3 complex-induced actin polymerization and induction of microspike formation by N-WASP. Proc. Natl. Acad. Sci. U.S.A. **97**, 12631–12636
42 Zalevsky, J., Lempert, L., Kranitz, H. and Mullins, R. D. (2001) Different WASP family proteins stimulate different Arp2/3 complex-dependent actin-nucleating activities. Curr. Biol. **11**, 1903–1913
43 Volkmann, N., Amann, K. J., Stoilova-McPhie, S., Egile, C., Winter, D. C., Hazelwood, L., Heuser, J. E., Li, R., Pollard, T. D. and Hanein, D. (2001) Structure of Arp2/3 complex in its activated state and in actin filament branch junctions. Science **293**, 2456–2459
44 Robinson, R. C., Turbedsky, K., Kaiser, D. A., Marchand, J. B., Higgs, H. N., Choe, S. and Pollard, T. D. (2001) Crystal structure of Arp2/3 complex. Science **294**, 1679–1684
45 Weaver, A., Heuser, J., Karginov, A., Lee, W., Parsons, J. and Cooper, J. (2002) Interaction of cortactin and N-wasp with arp2/3 complex. Curr. Biol. **12**, 1270–1278

Received 18 November 2002/3 January 2003; accepted 20 January 2003
Published as BJ Immediate Publication 20 January 2003, DOI 10.1042/BJ20021791

THE JOURNAL OF BIOLOGICAL CHEMISTRY
Vol. 278, No. 28, Issue of July 11, pp. 26086–26093, 2003
Printed in U.S.A.

Sequential Interaction of Actin-related Proteins 2 and 3 (Arp2/3) Complex with Neural Wiscott-Aldrich Syndrome Protein (N-WASP) and Cortactin during Branched Actin Filament Network Formation*

Received for publication, February 25, 2003, and in revised form, May 2, 2003
Published, JBC Papers in Press, May 5, 2003, DOI 10.1074/jbc.M301997200

Takehito Uruno‡, Jiali Liu‡, Yansong Li‡, Nicole Smith‡, and Xi Zhan‡§¶

From the ‡Department of Experimental Pathology, Jerome H. Holland Laboratory for the Biomedical Sciences, American Red Cross, Rockville, Maryland 20855 and the §Department of Cell Biology and Anatomy, The George Washington University, Washington D. C. 20037

The WASP and cortactin families constitute two distinct classes of Arp2/3 modulators in mammalian cells. Physical and functional interactions among the Arp2/3 complex, VCA (a functional domain of N-WASP), and cortactin were examined under conditions that were with or without actin polymerization. In the absence of actin, cortactin binds significantly weaker to the Arp2/3 complex than VCA. At concentrations of VCA 20-fold lower than cortactin, the association of cortactin with the Arp2/3 complex was nearly abolished. Analysis of the cells infected with *Shigella* demonstrated that N-WASP located at the tip of the bacterium, whereas cortactin accumulated in the comet tail. Interestingly, cortactin promotes Arp2/3 complex-mediated actin polymerization and actin branching in the presence of VCA at a saturating concentration, and cortactin acquired 20 nM affinity for the Arp2/3 complex during actin polymerization. The interaction of VCA with the Arp2/3 complex was reduced in the presence of both cortactin and actin. Moreover, VCA reduced its affinity for Arp2/3 complex at branching sites that were stabilized by phalloidin. These data imply a novel mechanism for the *de novo* assembly of a branched actin network that involves a coordinated sequential interaction of N-WASP and cortactin with the Arp2/3 complex.

Dynamic cortical actin assembly is intimately associated with membrane protrusions, cell crawling, phagocytosis, and intracellular vesicle trafficking. While assembly of actin bundles or cables requires formin-like proteins (1, 2), *de novo* actin polymerization in the cell cortex occurs primarily as the result of the function of actin-related proteins 2 and 3 (Arp2/3),[1] which form a stable protein complex with five other unique proteins (3–5). The Arp2/3 complex serves as a nucleation site for actin elongation, a major rate-limiting step in actin assembly (6–8), and forms distinct Y-shaped actin branches (9, 10). Branched actin network is a characteristic of cortical actin filaments found in cell leading edges such as lamellipodium, membrane ruffles, and membrane vesicles (11, 12). The formation of branched actin filaments is presumably the result of actin assembly at an Arp2/3 complex that binds to an existing actin filament (9, 13). However, the intrinsic actin nucleation activity of Arp2/3 complex is normally weak (9) and requires activation by binding to other cellular factors (6–8).

All Arp2/3 activators have been reported to bind to actin as well. The Arp2/3 activators can be categorized into two distinct classes based on their actin binding properties. Members of the first group bind to the monomeric form of actin (G-actin), and include the WASP family proteins (WASP, Ref. 14; N-WASP, Refs. 15 and 16; and SCAR/WAVE, Refs. 17 and 18 in metazoans; Las17 in yeast, Ref. 19), and ActA in *Listeria* (20). These proteins are able to activate the Arp2/3 complex by recruiting G-actin to the proximity of Arp2 and Arp3 subunits, resulting in a heterogeneous nucleation site for actin assembly (7). Members of the second group bind to filamentous actin (F-actin), and include the cortactin family proteins (cortactin, Refs. 21 and 22 and HS1, Ref. 23) in metazoans, and myosins-I (24–26) and Abp1 (27) in yeast. The ability of these proteins to promote actin assembly, however, appears to be modest compared with the WASP-related proteins, and the significance of such modest activations remains unclear.

Cortactin contains an N-terminal acidic domain that binds to the Arp2/3 complex and a central repeat domain consisting of 6.5 tandem repeats of unique 37 amino acids that binds to F-actin (21, 28, 29). Its C-terminal region contains a Src homology 3 (SH3) domain that associates with a variety of cellular proteins including CortBP1 (30), CBP90 (31), ZO-1 (32), and dynamin-2 (33). The structure of cortactin is well conserved in higher eukaryotes. Cortactin-like proteins have been also found in sea urchin, sponge, fruit fly, frog, chicken (35), mouse (36), and human (37), indicating an established function of cortactin at a very early stage of evolution. In contrast, no myosin I- or Abp1-like proteins that contain the acidic motif required for Arp2/3 binding have been found in mammalian cells (38). The only cortactin-related protein is HS1, a hematopoietic cell-specific protein, which also contains a similar N-terminal region, the repeat, and the C-terminal SH3 domains. The major difference between HS1 and cortactin is that HS1 has only 3.5 tandem repeats (23, 34).

While WASP proteins potentiate strongly the actin nucleation activity of the Arp2/3 complex, the branched filaments formed by WASP and the Arp2/3 complex are unstable and quickly undergo debranching by a mechanism that is still not clear (10, 39, 40). On the other hand, cortactin has a modest

* This work was supported by National Institutes of Health Research Grants RO1 HL52753-09, RO1 CA91984-01, Department of Defense Grant DAMD17-01-1-0125, and American Heart Association Established Investigator Grant 0040135N. The costs of publication of this article were defrayed in part by the payment of page charges. This article must therefore be hereby marked "*advertisement*" in accordance with 18 U.S.C. Section 1734 solely to indicate this fact.

¶ To whom correspondence should be addressed. Tel.: 301-738-0568; Fax: 301-738-0879; E-mail: zhanx@usa.redcross.org.

[1] The abbreviations used are: Arp2/3, actin-related proteins 2 and 3; BSA, bovine serum albumin; DAPI, diamidine-2-phyenyl indole; DTT, dithiothreitol; F-actin, filamentous actin; FITC, fluorescence isothiocyanate; GFP, green fluorescent protein; GST, glutathione *S*-transferase; PBS, phosphate-buffered saline; SH3, Src homology 3; VCA, verprolin-cofilin-acidic motif; N-WASP, neural Wiskott-Aldrich Syndrome protein.

activity for actin nucleation, but promotes significantly the formation of stable actin branches (22, 23). Despite these differences, WASP and cortactin bind to the Arp2/3 complex through a similar structural domain consisting of multiple acidic residues and a single tryptophan (7, 21). A recent study has reported that although both N-WASP and cortactin bind to the Arp3 subunit of the Arp2/3 complex (41), N-WASP binds to Arp2 and p41 subunits as well (41, 42). Interestingly, a cortactin fragment containing only the Arp2/3 binding domain competes poorly with N-WASP for the Arp2/3 complex even at a concentration 1000-fold higher than N-WASP (21, 41). Based on this finding, it has been suggested that a ternary complex of N-WASP, cortactin, and Arp2/3 might exist in the presence of excess amounts of cortactin, and the activities of WASP and cortactin might be synergistic for actin assembly under this condition (41). Indeed, both proteins have been implicated in the same actin-dependent cellular processes such as membrane ruffling (33, 43), podosome dynamics (35, 44), vesicle propulsion (45, 46), and actin comet tail formation by infectious agents (16, 47–49). However, there is evidence suggesting that cortactin may interact with the Arp2/3 complex in a mechanism distinct from N-WASP. For example, both cortactin and N-WASP are abundant proteins, and their cellular concentrations are in micromolar ranges (21, 50). It is also known that the majority of cortactin proteins are intimately associated with the Arp2/3 complex within cells (21). Thus, the precise role of cortactin and N-WASP and the nature of their functional relationship in actin assembly remain to be defined.

Here, we report that although the affinity of VCA, a constitutively active N-WASP peptide, for the Arp2/3 complex is much higher than that of cortactin in the absence of actin, such affinity is significantly reduced once actin polymerization is initiated. The release of VCA from the Arp2/3 complex is further promoted by the presence of cortactin, which apparently has increased its affinity for the activated Arp2/3 complex. Our data suggest that while N-WASP interacts primarily with the free form of the Arp2/3 complex, the more likely target for cortactin is the complex of Arp2/3 and F-actin at a branching site. Thus, we propose that the rapid formation of actin filaments requires a sequential event involving an initial activation of the Arp2/3 complex by N-WASP and a subsequent interaction between activated Arp2/3 complex and cortactin at the branching point.

EXPERIMENTAL PROCEDURES

Proteins—Murine cortactin tagged with 6× His at its C terminus was expressed in *Escherichia coli* and purified as described previously (21). Human N-WASP-derived VCA peptide tagged by GST was expressed and purified from *E. coli* as described (16) and further purified by Mono Q chromatography. For some experiments, GST-VCA was digested with thrombin at room temperature overnight, and the released tag-free VCA was further purified by Mono Q chromatography. GST-cort-(1–80), comprising the acidic domain and a region before the central repeat domain, and GST-cort-(1–375), containing both the acidic and the repeat domains, were expressed in *E. coli* and prepared as described (21). Bovine Arp2/3 complex was purified by a three-step procedure involving Q Sepharose ion-exchange, GST-VCA affinity chromatography and additional Q Sepharose chromatography (23). The protein in the flow-through fraction of the final Q Sepharose was concentrated by a Centricon 30 (Amicon), and the buffer of the sample was changed to 1× Ca^{2+}-free polymerization buffer (50 mM KCl, 2 mM $MgCl_2$, 1 mM EGTA, 0.25 mM ATP, 10 mM imidazole, pH 7.3, 3 mM NaN_3, and 0.5 mM dithiothreitol). Protein concentration was determined by the Bradford method using BSA as the standard.

GST Pull-down Assay—To measure the effect of VCA on the binding of cortactin to the Arp2/3 complex, 10 nM Arp2/3 complex was mixed with GST-cort-(1–80) or GST-cort-(1–375), and untagged VCA at different concentrations in a total 200-μl volume of 1× polymerization buffer. After a 15-min incubation at 22 °C, the reaction mixture was supplemented with BSA (1 mg/ml) and transferred to a 1.5-ml vial containing 20 μl of glutathione-Sepharose beads, and then incubated for 30 min with gentle rotation. The beads were pelleted by centrifugation at 300 × *g* for 1 min and subsequently subjected to SDS-PAGE followed by immunoblotting using anti-Arp3 polyclonal antibody (21). The blot was digitalized by film scanning and quantified by Scion Image software. The result was normalized based on five control samples of the Arp2/3 complex with different amounts on the same gel.

To measure the binding of VCA to the Arp2/3 complex during actin assembly, polymerization of 1.5 μM actin was initiated in the presence of 10 nM Arp2/3 complex, 100 nM GST-VCA, and cortactin at concentrations from 0 to 400 nM in 200 μl of 1× polymerization buffer for 30 min. The reaction mixture was then supplemented with BSA (1 mg/ml), and mixed with 20 μl of glutathione-Sepharose beads, and incubated for 30 min with gentle rotation. The beads were sedimented at 300 × *g* for 1 min, and the supernatant was transferred to a new 1.5-ml tube. 50 μl of the supernatant was mixed with an equal volume of 2× SDS sample buffer and boiled for 5 min. 16 μl of the sample was subjected to SDS-PAGE (12%) followed by transferring to a nitrocellulose membrane. Arp2/3 complex was detected by immunoblot analysis using Arp3 antibody.

Actin Polymerization—Polymerization of G-actin (10% pyrene-labeled, rabbit skeletal muscle actin from Cytoskeleton Inc.) was performed as described previously (21) with a modification. Briefly, Ca^{2+}-ATP-G-actin in G-actin buffer (5 mM Tris-HCl, pH 8.0, 0.2 mM $CaCl_2$, 0.2 mM ATP, and 0.5 mM DTT) was mixed with one-tenth volume of 10× exchange buffer (2 mM EGTA, 1 mM $MgCl_2$) for 3 min at 22 °C to convert to Mg^{2+}-ATP-G-actin. Polymerization was initiated by adding 60 μl of Mg^{2+}-ATP-G-actin (7.5 μM) to 240 μl of 1.25× polymerization buffer (62.5 mM KCl, 2.5 mM $MgCl_2$, 12.5 mM imidazole, pH 7.3, 1.25 mM EGTA, 0.125 mM $CaCl_2$, 0.625 mM DTT, 0.3125 mM ATP, and 3.75 mM NaN_3) containing Arp2/3 complex, GST-VCA, and cortactin at concentrations as indicated. The kinetics of actin polymerization was monitored by measuring the increase in pyrene fluorescence detected by an LS50B spectrophotometer (PerkinElmer Life Sciences) with filters for excitation at 365 nm and emission at 407 nm.

Fluorescence Microscopy Analysis of Branched Actin Filaments—The analysis was carried out essentially as described previously (10, 13). The specific conditions of actin polymerization for each experiment were described in the corresponding legends. Rhodamine-phalloidin (Molecular Probes) was added at the times indicated to actin polymerization reactions at a molar concentration equivalent to actin. After 5 min of incubation, the mixture was diluted 400-fold in fresh fluorescence buffer (100 mM KCl, 1 mM $MgCl_2$, 100 mM DTT, 10 mM imidazole, pH 7.3, 0.5% methylcellulose, 20 μg/ml catalase, 100 μg/ml glucose oxidase, and 3 mg/ml glucose). The diluted samples (2.4 μl) were applied onto cover slips precoated with 0.1% nitrocellulose in *n*-amyl acetate, and examined under an Olympus IX-70 inverted microscope using a ×100 objective lens with numerical aperture (NA) of 1.35. Images were captured by a charge-coupled device camera, and further processed on Adobe Photoshop to generate monochromatic images. The length of filaments and the number of branch points were measured by Scion Image software, and the degree of branching was calculated as the number of branches per micrometer of filament.

Immunofluorescence Analysis of Shigella-infected MDA-MB-231 Cells—Breast cancer MDA-MB-231 epithelial cells expressing GFP (enhanced green fluorescent protein) alone, GFP-N-WASP, or cortactin-GFP were prepared by retrovirus-mediated gene transfer according to the protocol described previously (51). Infection with *Shigella flexneri* M90T strain (a kind gift of C. Egile) was carried out according to the method described (52). Briefly, overnight culture of the bacteria was diluted in trypticase soy broth (BD Biosciences) at 1:100 and grown for 2 h at 37 °C to an OD_{600} = 0.2–0.3. Bacteria (100 bacteria/1 cell) were centrifuged at 3200 rpm for 4 min, rinsed twice with the cell growth medium (Dulbecco's modified Eagle's medium supplemented with 10% fetal bovine serum), and resuspended with the growth medium (2 ml/well). Cells, seeded on fibronectin-coated cover slips in a 6-well plate a day before infection, were washed once with the growth medium, overlaid with the bacterial suspension, and centrifuged at 2000 rpm for 10 min at 20 °C. Cells were incubated for 1 h at 37 °C to allow bacterial entry, then washed three times with the growth medium, and incubated in the medium containing 50 μg/ml of gentamicin for an additional 1–2 h at 37 °C before inspection.

Cells were fixed for 20 min in PBS containing 3.7% paraformaldehyde, incubated for 10 min in PBS-50 mM NH_4Cl twice to quench the fixative, and permeabilized in PBS containing 0.5% Triton X-100 for 10 min. The cells were blocked for 1 h with PBS containing 2% BSA, incubated with anti-GFP polyclonal antibody (Molecular Probes, 1:100), and anti-cortactin antibody (4F11; Upstate Biotechnology Inc., 1:100) for 1 h in PBS containing 0.2% BSA. After three washes with PBS, the

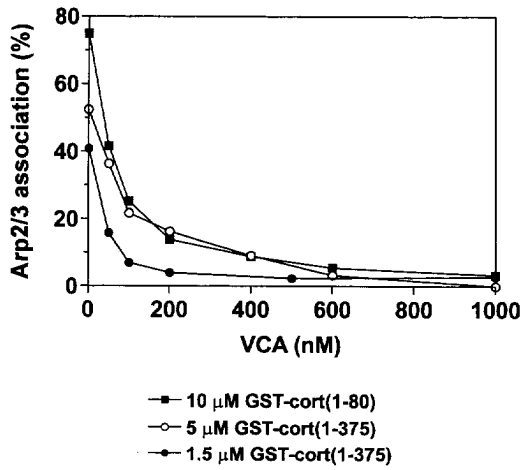

FIG. 1. **VCA inhibits the association of the Arp2/3 complex with cortactin in the absence of actin.** GST-cort-(1–375) at a final concentration of 1.5 μM (*filled circles*) or 5 μM (*open circles*), or 10 μM GST-cort-(1–80) (*filled squares*) was incubated with 10 nM Arp2/3 complex in the absence or presence of VCA at the indicated concentrations in 1× polymerization buffer (50 mM KCl, 2 mM $MgCl_2$, 10 mM imidazole, pH 7.3, 1 mM EGTA, 0.1 mM $CaCl_2$, 0.5 mM DTT, 0.25 mM ATP, and 3 mM NaN_3). After incubation for 15 min at 22 °C, the reaction mixture was supplemented with 1 mg/ml BSA, and GST-cortactin proteins and associated fractions were recovered by incubating with glutathione-Sepharose beads for 30 min followed by brief centrifugation. The presence of Arp2/3 complex in the beads fraction was detected by immunoblotting using anti-Arp3 antibody. The bands corresponding to Arp3 were digitalized by film scanning, and the density of each band was quantified by Scion Image software and normalized based on Arp2/3 complex samples of five different concentrations loaded on the same gel. The percentage of the normalized values for each sample in relation to the total amount of Arp2/3 in the reaction was plotted as a function of VCA concentration.

cells were further incubated with FITC-labeled anti-rabbit IgG antibody (1:50) and rhodamine-labeled anti-mouse IgG antibody (1:50) in PBS containing 0.2% BSA for 1 h. The cells were then incubated with diamidine-2-phenyl indole (DAPI) (10 μg/ml) for 5 min and washed three times with PBS. The stained cover slips were mounted on a glass slide with 20 μl of Prolong Antifade preservative (Molecular Probes) and sealed with nail polish. The cells were examined under an Olympus IX-70 inverted microscope using a ×60, NA = 1.25 objective lens.

RESULTS

N-WASP-VCA Inhibits the Association of Cortactin with Arp2/3 Complex in the Absence of Actin—In an effort to understand the relationship of N-WASP and cortactin during actin assembly, we examined whether the two types of Arp2/3 activators could bind simultaneously to the Arp2/3 complex. As a result, the interaction of cortactin and Arp2/3 complex was examined in the presence of a VCA peptide derived from human N-WASP (16) by pull-down analysis with murine cortactin recombinant proteins GST-cort-(1–80) and GST-cort-(1–375), both of which have a similar affinity for the Arp2/3 complex with a K_d of about 1 μM (21). As shown in Fig. 1, GST-cort-(1–375) was able to pull-down 41% of 10 nM Arp2/3 complex at 1.5 μM, and 52% at 5 μM, in the absence of VCA. However, this ability to pull-down the Arp2/3 complex was dramatically inhibited by VCA in a dose-dependent manner and nearly abolished by VCA at concentrations significantly lower than GST-cort-(1–375). (200 nM VCA abolished the association of Arp2/3 complex with 1.5 μM cortactin protein, and 600 nM VCA abolished that with 5 μM cortactin.) Binding of GST-cort-(1–80) to the Arp2/3 complex was also inhibited by VCA in a similar manner (Fig. 1). With either of the cortactin proteins, VCA inhibited 50% of cortactin binding to the Arp2/3 complex at ~50 nM. This result is consistent with the previously reported relative affinities of VCA and cortactin for the Arp2/3 complex: VCA has a K_d value from 0.1 to 0.2 μM (16, 21, 23), and cortactin has a K_d from 0.7 to 1.3 μM (21, 23, 29, 41). Our finding also agrees with a recent report showing that a similar cortactin peptide encoding the N-terminal region (1–80) competed poorly with VCA in GST pull-down assays (41).

Cortactin and N-WASP Localize in Distinct Areas in the Comet Tail Induced by S. flexneri—The above data suggest that binding of cortactin and VCA to Arp2/3 complex is mutually exclusive, making it less likely that they form a ternary complex with the Arp2/3 complex as previously suggested (41). To further confirm this notion, we examined the distribution of cortactin and N-WASP in the actin comet tail formed by the infectious agent *S. flexneri* in the cytoplasm of epithelial cells expressing human N-WASP fused with GFP (GFP-N-WASP). It has been shown that *Shigella* protein IcsA at the bacterial surface is able to interact with and activate N-WASP, which in turn activates Arp2/3 complex-mediated actin assembly to induce comet tails (16). The bacteria were stained with DAPI, a DNA binding dye (blue); and GFP-N-WASP and cortactin were stained with anti-GFP (green) and cortactin (red) antibodies, respectively. Although both GFP-N-WASP and cortactin were found in the comet tails, two proteins displayed distinct localization profiles in relation to bacteria (Fig. 2). N-WASP was predominantly localized at either one or both polar ends of the bacterial surface (Fig. 2, *arrowheads*). This observation is consistent with previous reports (16, 48). In contrast, cortactin was primarily associated with the entire tail (Fig. 2, *arrows*), where Arp2/3 complex is known to be abundant (16). Colocalization of GFP-N-WASP and cortactin was found, if any, only in a narrow region where the bacterial head and comet tail meet. Thus, it appears that N-WASP is closely associated with the initiation site for actin assembly while cortactin is stably associated with Arp2/3 complex and the more established actin network. Similar distribution pattern of the two proteins was also reported for the actin comet tail induced by vaccinia virus (53).

Cortactin Is Able to Promote Actin Polymerization in the Presence of VCA at Saturating Concentrations—To further explore the specific role of VCA and cortactin in actin polymerization mediated by the Arp2/3 complex, we examined Arp2/3 complex-mediated actin assembly in the presence of both cortactin and GST-VCA. At low concentrations of the Arp2/3 complex (~10 nM), which showed very little intrinsic nucleation activity, cortactin had no significant effect on the activation of the complex even at 500 nM until GST-VCA was added (data not shown), suggesting a synergistic function between cortactin and VCA (21, 22). To understand better the nature of this synergistic function, we analyzed the ability of cortactin to promote actin polymerization in the presence of 1 μM GST-VCA. Since GST-VCA has a 100 nM affinity for the Arp2/3 complex, and 1 μM VCA was able to abolish binding of 10 μM cortactin to the Arp2/3 complex (Fig. 1), it was assumed that 1 μM GST-VCA would have saturated the binding sites on 8 nM Arp2/3 complex available for cortactin. Surprisingly, under this condition cortactin was still able to provoke a strong actin assembly even at concentrations as low as 5 nM (Fig. 3*A*). A dose dependence analysis with various concentrations of GST-VCA further demonstrated that cortactin induces consistently a half-maximal stimulation at ~20 nM (Fig. 3*B* and Refs. 21 and 23), indicating that this value reflects a biochemical property of cortactin independent of GST-VCA. The similar result was also obtained with untagged VCA (data not shown). Therefore, it appears that cortactin promotes actin polymerization in a unique mechanism that apparently requires neither the formation of a complex with N-WASP nor a competition with N-WASP for Arp2/3 binding. Previous studies have demonstrated that cortactin stimulates actin polymerization in a

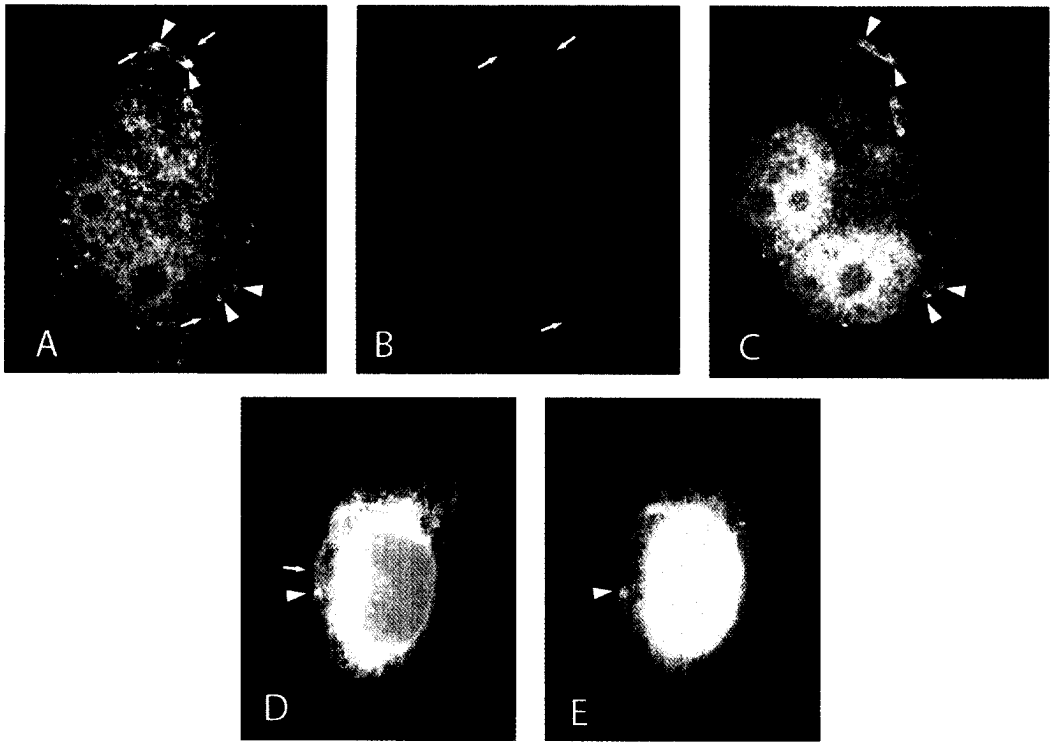

FIG. 2. **Distinct localization of N-WASP and cortactin in the comet tails induced by *S. flexneri*.** MDA-MB-231 epithelial cells expressing GFP-N-WASP were infected with *S. flexneri* M90T strain, and the localization of GFP-N-WASP (*green*) and cortactin (*red*) in the comet tail induced by the bacteria was analyzed by immunofluorescent staining using anti-GFP and anti-cortactin antibodies, respectively. Host and bacterial nuclei (*blue*) were stained with DAPI. *Panels A* to *C* show examples of GFP-N-WASP (*arrowheads*) associated at both ends of a bacterium with either a double or a single cortactin tail (*arrows*). *Panels D* and *E* show examples of GFP-N-WASP (*green*, *arrowheads*) found at the posterior tip of a bacterium with a single cortactin tail (*red*, *arrow*).

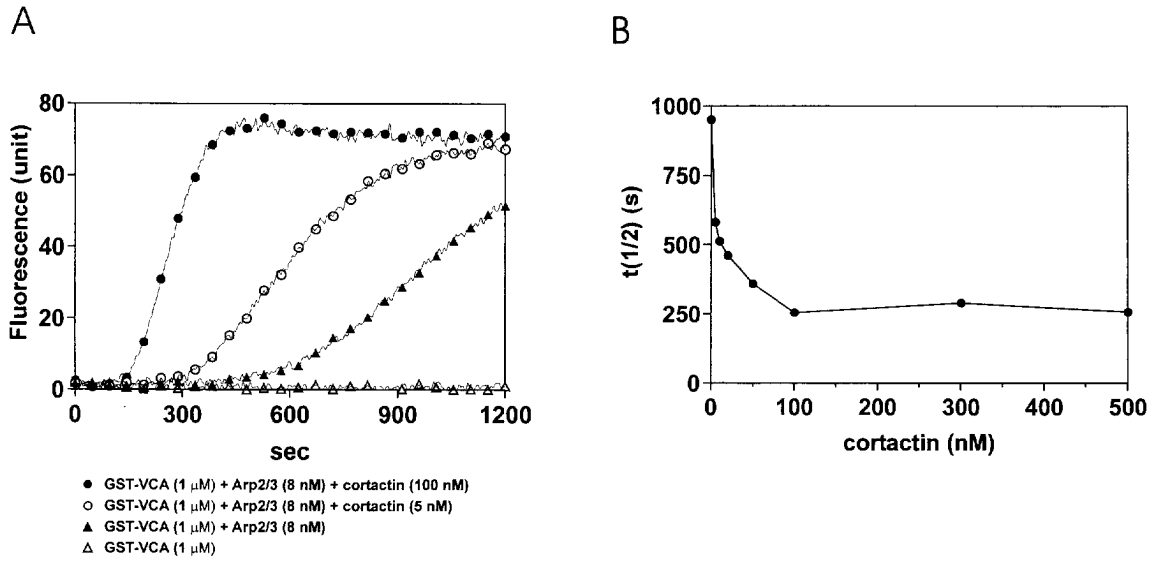

FIG. 3. **Cortactin stimulates actin nucleation by the Arp2/3 complex in the presence of GST-VCA at a saturating concentration.** *A*, kinetics of actin polymerization in the presence of 1 μM GST-VCA. Polymerization of 1.5 μM pyrene-labeled actin was recorded over time in the presence of 1 μM GST-VCA with or without 8 nM Arp2/3 complex and cortactin at 0, 5, or 100 nM, respectively. *B*, dose dependence of the stimulation of VCA-Arp2/3 complex-mediated actin polymerization by cortactin. Actin polymerization was performed under the same condition as described for *A*, except a broader range (from 1 to 500 nM) of cortactin concentrations was used. The time required to reach half-maximal polymerization ($t_{1/2}$) was calculated from each polymerization curve and is presented as a function of cortactin concentration.

Arp2/3 binding-dependent manner (21, 22), indicting that 20 nM concentration for a half-maximum stimulation likely reflects the affinity of cortactin for the Arp2/3 complex during actin assembly.

Cortactin Induces the Release of VCA from the Arp2/3 Complex through the Formation of Branched Actin Filaments—The above observations led us to hypothesize that the relative affinities of VCA and cortactin for the Arp2/3 complex might have been changed during the course of actin polymerization. To test this possibility, we first examined the interaction of VCA and the Arp2/3 complex by pull-down analysis under the conditions where actin polymerization was involved. Actin polymerization was initiated in the presence of GST-VCA and the Arp2/3 complex with or without cortactin. After 30 min when actin polymerization was completed, the reaction mixture was incubated with glutathione beads to pull-down GST-VCA and the

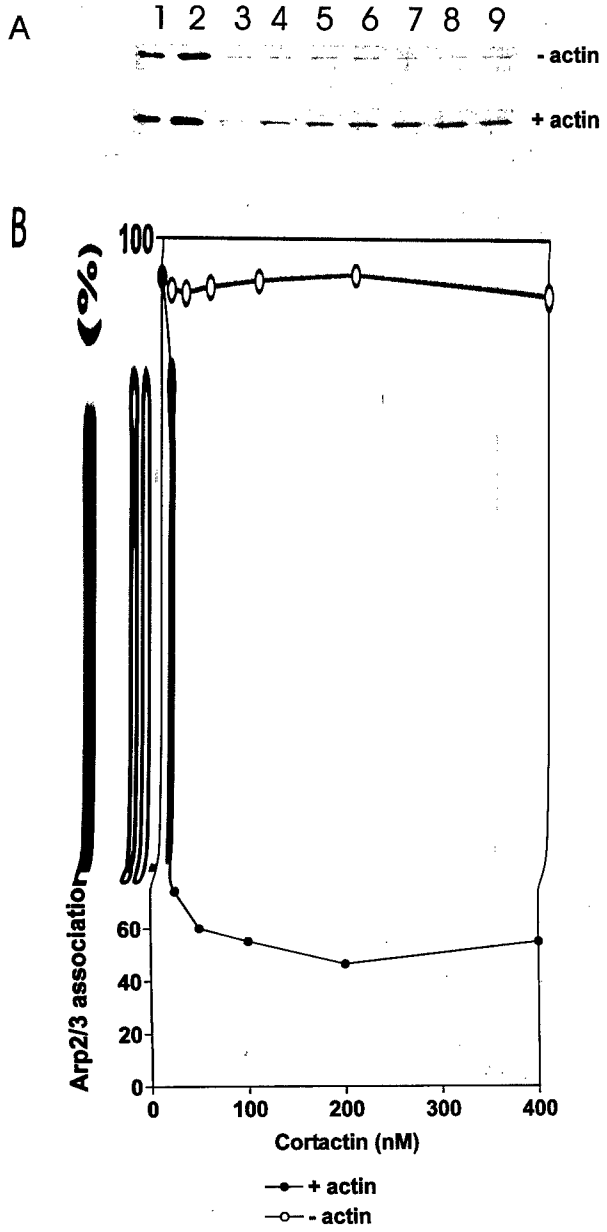

FIG. 4. **Cortactin induces dissociation of Arp2/3 complex from VCA under the condition for actin polymerization.** *A*, analysis of VCA-associated Arp2/3 complex during actin polymerization. GST-VCA (100 nM) and Arp2/3 complex (10 nM) was preincubated with or without cortactin at the indicated concentrations for 3 min. G-actin (1.5 μM) was added to the mixture to initiate actin polymerization in a final volume of 200 μl of 1× polymerization buffer at 22 °C. In the control experiment (−actin), the G-actin buffer alone was added. After 30 min of polymerization, the reaction mixture was supplemented with BSA (1 mg/ml) and mixed with 20 μl of glutathione beads. The beads were pelleted by centrifugation. The supernatant fractions were subjected to SDS-PAGE followed by immunoblotting using anti-Arp3 antibody. The bands corresponding to Arp3 were digitalized by film scanning. *Lane 1*, half the amount of the sample on *lane 2*; *lane 2*, 0 nM GST-VCA and cortactin; *lane 3*, 100 nM GST-VCA, 0 nM cortactin; *lanes* 4–9, 100 nM GST-VCA plus 10, 25, 50, 100, 200, and 400 nM cortactin, respectively. *B*, the quantification of the release of Arp2/3 complex from VCA. The digitalized image of the blot as shown in *A* was quantified using Scion Image. The Arp2/3 complex associated with GST-VCA was estimated by subtracting that in the supernatant from the total amount in the reaction and plotted as a function of cortactin concentration.

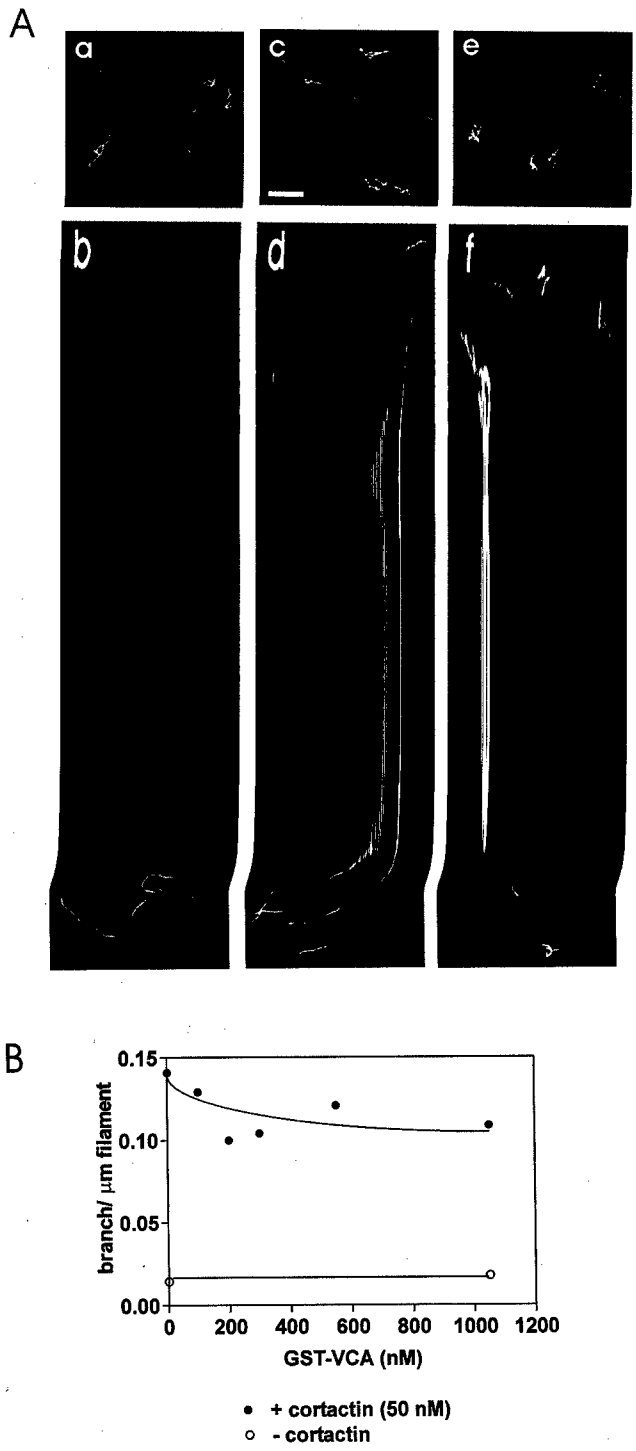

FIG. 5. **VCA is unable to inhibit actin branching activity of cortactin.** *A*, actin (1.5 μM) was polymerized in the presence of 100 nM GST-VCA and 10 nM Arp2/3 complex with (*a* and *c*) or without (*b* and *d*) 50 nM cortactin in a total 300-μl volume of reaction. After 15 min of polymerization, 45 μl of the reaction was transferred to a new tube containing either 5 μl of 1× polymerization buffer (*a* and *b*) or 5 μl of 10 μM GST-VCA (*c* and *d*, the final concentration was 1.1 μM), and incubated for additional 45 min. Actin branching was then examined by fluorescence microscopy. *Panels e* and *f* are the samples for actin branching at 3 min after polymerization initiation in the presence (*e*) or absence (*f*) of 50 nM cortactin. *Bar* in *panel c* indicates a 5-μm length. *B*, actin polymerization was performed as above and GST-VCA at a series of concentrations was added after 15 min of polymerization. The degree of actin branching was calculated by counting the number of branching points from actin filaments of 200 μm or longer in length and expressed as branch per μm length filament. The value of actin branching was then plotted as a function of GST-VCA concentration.

associated Arp2/3 complex. The Arp2/3 complex remaining in the supernatant was analyzed by immunoblotting of the Arp3 subunit (Fig. 4*A*). In the absence of cortactin GST-VCA was able to pull-down more than 90% of the Arp2/3 complex with or without adding actin (Fig. 4*A*, *lane 3*; Fig. 4*B*, at 0 nM cortactin). In the presence of cortactin and actin, the ability of GST-VCA to pull-down Arp2/3 was altered. Under this condition, the

and the Arp2/3 complex and GST-VCA to a steady state, and additional GST-VCA was added afterward to the reaction to compete for Arp2/3 binding. The actin branching was then

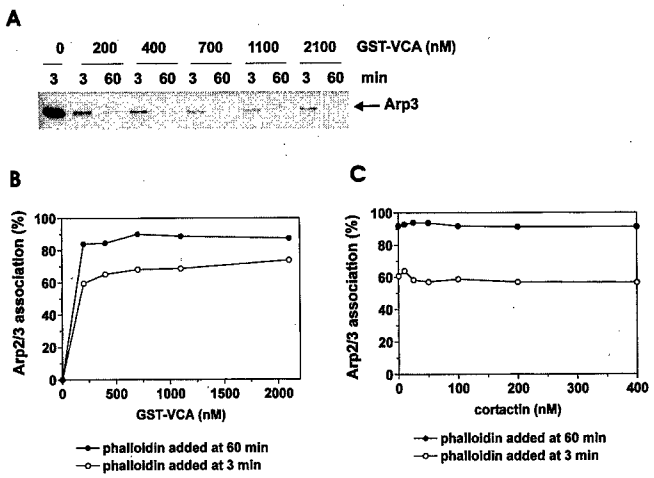

FIG. 6. **GST-VCA is unable to associate with Arp2/3 complex in branched actin filaments.** *A*, effect of actin branching on the association of VCA with Arp2/3 complex. GST-VCA (100 nM) and Arp2/3 complex (10 nM) were preincubated for 3 min at 22 °C. G-actin (1.5 μM) was added to the mixture to initiate polymerization in a final volume of 200 μl of 1× polymerization buffer. After 3 or 60 min, 1.5 μM phalloidin was added to the reaction, incubated for 3 min, and additional GST-VCA was added at final concentrations of 200, 400, 700, 1100, and 2100 nM, respectively. The amount of Arp2/3 complex that was not associated with GST-VCA was determined by immunoblotting of Arp3 present in the supernatant after GST-VCA precipitation. *B*, quantification of the effect of actin branching on the association of Arp2/3 complex with VCA. Arp2/3 complex association as analyzed in *A* was calculated based on the difference between the density of Arp3 band in the supernatant and that in the control sample without GST-VCA. The percentage of the association was estimated by comparison to that in the control sample and further plotted as a function of the concentration of GST-VCA. *C*, effect of actin branching on the cortactin-mediated inhibition of VCA binding to the Arp2/3 complex. Actin polymerization was performed as described above. After 3 or 60 min of initiation, the actin filaments were fixed by adding 1.5 μM phalloidin and incubation for 3 min. Cortactin was then added to the reaction mixtures at the indicated concentrations. After an additional 15 min of incubation, the reaction mixtures were subjected to GST-VCA precipitation, and the supernatants were subjected to SDS-PAGE followed by immunoblotting using anti-Arp3 antibody. The amount of the Arp2/3 complex associated with GST-VCA was estimated as described above.

replacing cortactin associated with Arp2/3 complex on the branched actin filaments that have been already established.

VCA Reduces Its Affinity for the Arp2/3 Complex at Branched Actin Filaments—Cortactin inhibited maximally only 50% of the binding of the Arp2/3 complex to GST-VCA (Fig. 4). The remaining bound Arp2/3 complex could be in the F-actin-free form to which cortactin binds weakly compared with GST-VCA. These Arp2/3 complexes in the free form might be either released from F-actin as a result of a debranching process (54) or those that did not participate in actin nucleation. To verify that VCA may only bind to the free form of Arp2/3 complex and may acquire a relatively lower affinity than cortactin for Arp2/3 complex once it is associated with F-actin, we examined the interaction of GST-VCA with the Arp2/3 complex at branched actins in the absence of cortactin. Previous studies have shown that branched actin filaments initiated by the Arp2/3 complex can be also stabilized by fixation with phalloidin (10, 54). Thus, we analyzed the interaction of VCA with the Arp2/3 complex in the presence of phalloidin that was added at either 3 or 60 min after nucleation of actin assembly. Actin filaments formed under each condition displayed different degrees of actin branching. At 3 min, many actin filaments remained branched, indicating that a significant portion of the Arp2/3 complex was still at actin branches (Fig. 5*A*, *panel f*). On the other hand, the most branched actin filaments had undergone debranching at 60 min (Fig. 5*A*, *panel b*), and the majority of the Arp2/3 complex was assumed to be in the free form. When GST-VCA was precipitated from the actin assembly reaction fixed at 3 min with glutathione beads, only 60% of the Arp2/3 complex was able to be pulled down (Fig. 6, *A* and *B*). In contrast, nearly 90% of the Arp2/3 complex was pulled-down by GST-VCA at 60 min. The efficiency of pull-down at 60 min was the same as that observed without phalloidin and cortactin (Fig. 4) where most branched actin filaments have been debranched. Thus, the ability of GST-VCA to interact with the Arp2/3 complex is apparently inversely correlated with the degree of actin branching. In addition, the pull-down of the Arp2/3 complex by GST-VCA reached a maximum level at concentrations as low as 250 nM (Fig. 6*B*) at either 3 or 60 min, suggesting that the remaining Arp2/3 complex, which was likely associated with branched F-actin, was unable to be accessed by GST-VCA even at high concentrations. Indeed, when the similar assay was performed in the presence of cortactin that was added after phalloidin fixation, cortactin was no longer able to inhibit the interaction between GST-VCA and the Arp2/3 complex (Fig. 6*C*), indicating that the Arp2/3 complex associated with GST-VCA was in the free form for which cortactin had a much lower affinity than VCA (Fig. 1). Taken together, these results suggest that VCA had reduced its affinity for the Arp2/3 complex on the branched F-actin.

DISCUSSION

In this study, we provide evidence for dramatic changes in the relative affinities of N-WASP and cortactin for the Arp2/3 complex during the course of actin assembly. Although N-WASP shows predominance for the free form of the Arp2/3 complex, it appears that cortactin has a much higher affinity for the Arp2/3 complex once it is incorporated into actin filaments. First, cortactin promotes significantly Arp2/3-mediated actin nucleation even in the presence of VCA at a concentration 200-fold higher than cortactin that would have occupied all the binding sites of the Arp2/3 complex for cortactin. Based on the analysis of actin nucleation and actin branching (21, 23) (also in this study), we estimated the affinity of cortactin for the Arp2/3 complex at ~20 nM, which is significantly lower than 0.7–1.3 μM for the free form of Arp2/3 as reported previously (21, 23, 29, 41). Second, the interaction between VCA and the Arp2/3 complex becomes much weaker in the presence of cortactin and actin. In fact, by analysis of binding to the Arp2/3 complex in the presence of phalloidin or cortactin, VCA appears to bind to only those Arp2/3 complexes that are in the free form released from debranching. Finally, VCA is not able to displace cortactin from the Arp2/3 complex at branching sites of actin filaments.

Reduced affinity of WASP for the Arp2/3 complex after actin nucleation is initiated has been postulated because of a presumed requirement for a rapid motility driven by actin polymerization (16, 55). It has been reported that the Arp2/3 complex requires hydrolysis of ATP for actin nucleation (55, 56), and VCA prefers ATP-bound Arp2/3 complex with a 140 nM affinity to the ADP-bound form with a 0.7 μM affinity (55). Thus, the function of VCA may be to place an actin monomer in contact with an Arp2/3 complex and stimulate ATP hydrolysis. Hydrolysis of ATP to an ADP-P_i state would then cause a conformational change that allows Arp2, Arp3, and an actin monomer to associate and form a nucleus, and subsequent release of VCA from the Arp2/3 complex. In this study, we have directly observed the reduced binding of VCA to the Arp2/3 complex, which was only apparent when actin polymerization took place in the presence of cortactin. Although the measurement was carried out when actin polymerization was completed, fixation of actin polymerization by phalloidin at different times has mimicked the function of cortactin to stabilize actin branching

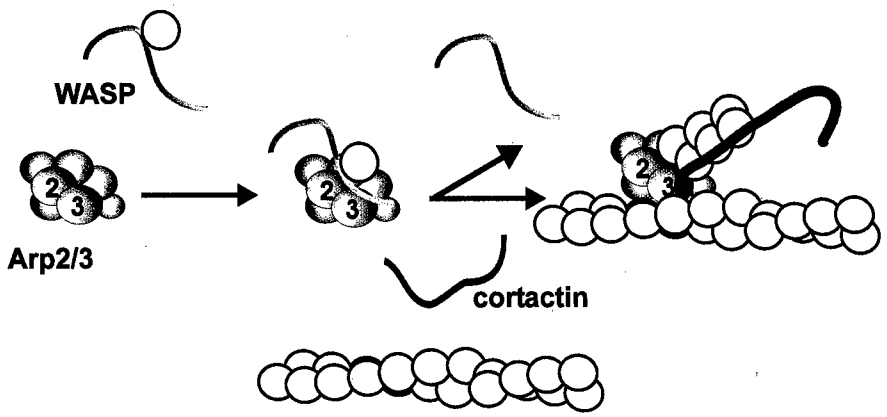

FIG. 7. **A model for the formation of de novo branched actin filaments mediated by Arp2/3 complex, N-WASP, and cortactin.** In *de novo* actin assembly, N-WASP acquires a high affinity for the free form of Arp2/3 complex upon stimulation by membrane-associated signaling molecules such as Cdc42 and phosphatidylinositol 4,5-bisphosphate. The association with N-WASP leads to activation of the Arp2/3 complex, facilitation of its binding to an existing actin filament, and initiation of new actin assembly. At this stage, the activated Arp2/3 complex becomes less accessible to N-WASP but is more prone to the association with cortactin, which binds to both the Arp2/3 complex and the nascent actin filament with an affinity 50-fold higher than for the free form of Arp2/3 complex. The complex of cortactin/Arp2/3/F-actin at the branching site is stable and serves as a better nucleation site for assembly of branched actin filaments.

and demonstrated that the change in the affinity of VCA for the Arp2/3 complex occurs at an early phase of actin assembly. Since phalloidin is known to stabilize actin-associated ADP-P_i (57), an intermediate form from the transition from ATP to ADP, our finding supports the view that hydrolysis of ATP hydrolysis contributes to the change in the affinity of VCA for the Arp2/3 complex. However, given a dramatic increase in the affinity of cortactin from 1 μM to 20 nM, which is even stronger than VCA for ATP-bound Arp2/3 complex, cortactin could play an important role in the dissociation of VCA from the Arp2/3 complex in a manner independent of ATP hydrolysis.

The enhanced affinity of cortactin for Arp2/3 complex during actin assembly could be a result of a substantial conformational change in the Arp2/3 complex (58, 59). However, this structural change could not be simply due to VCA binding because it only occurs when actin is present. Indeed, GST-cort-(1–80) fusion protein, which has the same affinity for the free form of the Arp2/3 complex as intact cortactin (21), is not able to induce actin polymerization or branching, nor inhibit the activity of an intact cortactin (data not shown). Thus, the Arp2/3 complex itself, whether it is in the activated form or not, is not sufficient to account for the increase in its affinity for cortactin during actin polymerization. It is more likely that the acquired high affinity of cortactin for Arp2/3 complex reflects its interaction with both Arp2/3 complex and actin filament at the branching site. In fact, cortactin is known as a potent F-actin binding protein with an affinity from 0.2 to 0.4 nM (21, 28). Our recent measurements using freshly polymerized actin fixed with phalloidin estimated a K_d value even below 100 nM (23). The alignment of activated Arp2/3 complex with a daughter filament may further enhance the affinity of cortactin. Additional evidence supporting this possibility is a previous observation that cortactin absolutely requires its binding to F-actin for its ability to promote actin nucleation and actin branching (21, 22).

Because of its strong dependence on F-actin binding, we propose a model for a possible interaction between cortactin and Arp2/3 complex at a nucleation site as shown in Fig. 7. In this model, N-WASP activates the Arp2/3 complex by a transient interaction, which results in changes in the configuration of the Arp2/3 complex and increase in the association of the Arp2/3 complex with an existing actin filament (60). Once the branching point is established, N-WASP may be released from the complex as a result of either ATP hydrolysis or replacement by cortactin, which has acquired a much higher affinity for the branching point. Since both WASP-related proteins and cortactin are abundantly present in most cells (21), a high affinity of the WASP family proteins for the Arp2/3 complex, 100–200 nM with N-WASP (16, 21) and 400 nM with WAVE (61, 62), would secure an instant activation of the free form of the Arp2/3 complex in a *de novo* actin assembly. Similarly, the high affinity of cortactin for the activated Arp2/3 complex would be necessary to facilitate the release of WASP from the branching site of actin filaments and to increase stabilized nucleation sites for a rapid growth of actin filaments. Consequently, the sequential reaction will result in a robust polymerization of branched actin network upon stimulation. Supporting evidence for this novel mechanism for actin polymerization is the observation that cortactin, which itself may not directly activate the free form of the Arp2/3 complex as N-WASP does, can potently stimulate both actin nucleation and actin branching (Fig. 3).

Our conclusion is significantly different from a recent report (41) that VCA and cortactin may bind simultaneously to the Arp2/3 complex via different subunits and form a ternary complex with Arp2/3 complex. The apparent discrepancy is at least partially due to different conditions used in their experimental procedure, which was performed with a cortactin fragment containing only the Arp2/3 binding domain and lacking the activity for either actin nucleation or branching. Although the report has described a competition between VCA and the cortactin fragment and the authors indicated the presence of a common binding site at the Arp3 subunit for both types of protein, no clear conclusion was drawn because of a further finding that the cortactin N-terminal peptide could not compete with the VCA binding sites at Arp2 and p41 sites of the free form of the Arp2/3 complex (41). While our study using fully functional cortactin proteins does not rule out the possibility that N-WASP might still associate with p41 and Arp2 subunits in the presence of cortactin, this possibility is very unlikely under the condition when actin polymerization takes place, given the fact that their relative affinities have been dramatically changed. Consistent with our conclusion, cortactin and N-WASP do not appear to be co-localized in the *Shigella*-induced actin comet tail that is composed of newly formed branched actin network driven by constitutively activated N-WASP and Arp2/3 complex (16, 63). However, cortactin could be colocalized more closely with WASP family proteins in other cellular systems. For example, cortactin is a primary substrate of the Src protein tyrosine kinases (35, 64) and binds to several membrane-associated proteins including dynamin-2, ZO-1, and CortBP1 via its SH3 domain (30, 32, 33, 65). Thus, cortactin is

likely to function in proximity to the plasma and other intracellular membranes as well. Indeed, cortactin is abundantly present in lamellipodium, membrane ruffles, and endosomes (21, 35, 46, 66). By interacting with different components on the membrane, cortactin and N-WASP likely play an important role in the organization of actin network by fine-tuning the size and branches of actin filaments to power movements of particular types of cellular organelles.

It is also possible that WASP-like proteins may facilitate the association of cortactin with the Arp2/3 complex during actin assembly. In fact, it has been reported that cortactin could bind to N-WASP directly though the cortactin SH3 domain (44). A recent study has also described an interaction between cortactin and WIP, a WASP interacting protein (67). Thus, WASP could also affect cortactin through indirect interaction. While the actin branching activity of cortactin as analyzed *in vitro* does not appear to require the function of its SH3 domain (data not shown) and the VCA fragment used in this study does not contain an apparent SH3 binding domain, a transient interaction with WASP proteins could contribute to recruitment of cortactin to the sites for cortical actin assembly in cells. Since many cellular proteins have also been found to bind to the cortactin SH3 domain, distinguishing specific roles of these proteins in the function of cortactin/WASP/Arp2/3-mediated cortical actin assembly may eventually provide a detailed mechanism for regulating and directing actin assembly in cells.

Acknowledgments—We thank C. Egile and M. B. Goldberg (Harvard Medical School) for technical help with *Shigella* infection. We also thank Jeff Winkles for the critical reading; and Jian-Jiang Hao, Jianwei Zhu and Kang Zhou for helpful discussions with this work.

REFERENCES

1. Pruyne, D., Evangelista, M., Yang, C., Bi, E., Zigmond, S., Bretscher, A., and Boone, C. (2002) *Science* **297,** 612–615
2. Sagot, I., Rodal, A. A., Moseley, J., Goode, B. L., and Pellman, D. (2002) *Nat. Cell Biol.* **4,** 626–631
3. Machesky, L. M., Atkinson, S. J., Ampe, C., Vandekerckhove, J., and Pollard, T. D. (1994) *J. Cell Biol.* **127,** 107–115
4. Welch, M. D., DePace, A. H., Verma, S., Iwamatsu, A., and Mitchison, T. J. (1997) *J. Cell Biol.* **138,** 375–384
5. Mullins, R. D., Stafford, W. F., and Pollard, T. D. (1997) *J. Cell Biol.* **136,** 331–343
6. Pollard, T. D., Blanchoin, L., and Mullins, R. D. (2000) *Annu. Rev. Biophys. Biomol. Struct.* **29,** 545–576
7. Higgs, H. N., and Pollard, T. D. (2001) *Annu. Rev. Biochem.* **70,** 649–676
8. Welch, M. D., and Mullins, R. D. (2002) *Annu. Rev. Cell Dev. Biol.* **18,** 247–288
9. Mullins, R. D., Heuser, J. A., and Pollard, T. D. (1998) *Proc. Natl. Acad. Sci. U. S. A.* **95,** 6181–6186
10. Blanchoin, L., Amann, K. J., Higgs, H. N., Marchand, J. B., Kaiser, D. A., and Pollard, T. D. (2000) *Nature* **404,** 1007–1011
11. Borisy, G. G., and Svitkina, T. M. (2000) *Curr. Opin. Cell Biol.* **12,** 104–112
12. Bailly, M., Macaluso, F., Cammer, M., Chan, A., Segall, J. E., and Condeelis, J. S. (1999) *J. Cell Biol.* **145,** 331–345
13. Amann, K. J., and Pollard, T. D. (2001) *Nat. Cell Biol.* **3,** 306–310
14. Yarar, D., To, W., Abo, A., and Welch, M. D. (1999) *Curr. Biol.* **9,** 555–558
15. Rohatgi, R., Ma, L., Miki, H., Lopez, M., Kirchhausen, T., Takenawa, T., and Kirschner, M. W. (1999) *Cell* **97,** 221–231
16. Egile, C., Loisel, T. P., Laurent, V., Li, R., Pantaloni, D., Sansonetti, P. J., and Carlier, M. F. (1999) *J. Cell Biol.* **146,** 1319–1332
17. Machesky, L. M., Mullins, R. D., Higgs, H. N., Kaiser, D. A., Blanchoin, L., May, R. C., Hall, M. E., and Pollard, T. D. (1999) *Proc. Natl. Acad. Sci. U. S. A.* **96,** 3739–3744
18. Suetsugu, S., Miki, H., and Takenawa, T. (1999) *Biochem. Biophys. Res. Commun.* **260,** 296–302
19. Winter, D., Lechler, T., and Li, R. (1999) *Curr. Biol.* **9,** 501–504
20. Welch, M. D., Rosenblatt, J., Skoble, J., Portnoy, D. A., and Mitchison, T. J. (1998) *Science* **281,** 105–108
21. Uruno, T., Liu, J., Zhang, P., Fan, Y., Egile, C., Li, R., Mueller, S. C., and Zhan, X. (2001) *Nat. Cell Biol.* **3,** 259–266
22. Weaver, A. M., Karginov, A. V., Kinley, A. W., Weed, S. A., Li, Y., Parsons, J. T., and Cooper, J. A. (2001) *Curr. Biol.* **11,** 370–374
23. Uruno, T., Zhang, P., Liu, J., Hao, J. J., and Zhan, X. (2003) *Biochem. J.* **371,** 485–493
24. Lee, W. L., Bezanilla, M., and Pollard, T. D. (2000) *J. Cell Biol.* **151,** 789–800
25. Evangelista, M., Klebl, B. M., Tong, A. H., Webb, B. A., Leeuw, T., Leberer, E., Whiteway, M., Thomas, D. Y., and Boone, C. (2000) *J. Cell Biol.* **148,** 353–362
26. Lechler, T., Shevchenko, A., and Li, R. (2000) *J. Cell Biol.* **148,** 363–373
27. Goode, B. L., Rodal, A. A., Barnes, G., and Drubin, D. G. (2001) *J. Cell Biol.* **153,** 627–634
28. Wu, H., and Parsons, J. T. (1993) *J. Cell Biol.* **120,** 1417–1426
29. Weed, S. A., Karginov, A. V., Schafer, D. A., Weaver, A. M., Kinley, A. W., Cooper, J. A., and Parsons, J. T. (2000) *J. Cell Biol.* **151,** 29–40
30. Boeckers, T. M., Kreutz, M. R., Winter, C., Zuschratter, W., Smalla, K. H., Sanmarti-Vila, L., Wex, H., Langnaese, K., Bockmann, J., Garner, C. C., and Gundelfinger, E. D. (1999) *J. Neurosci.* **19,** 6506–6518
31. Ohoka, Y., and Takai, Y. (1998) *Genes Cells* **3,** 603–612
32. Katsube, T., Takahisa, M., Ueda, R., Hashimoto, N., Kobayashi, M., and Togashi, S. (1998) *J. Biol. Chem.* **273,** 29672–29677
33. McNiven, M. A., Kim, L., Krueger, E. W., Orth, J. D., Cao, H., and Wong, T. W. (2000) *J. Cell Biol.* **151,** 187–198
34. Kitamura, D., Kaneko, H., Taniuchi, I., Akagi, K., Yamamura, K., and Watanabe, T. (1995) *Biochem. Biophys. Res. Commun.* **208,** 1137–1146
35. Wu, H., Reynolds, A. B., Kanner, S. B., Vines, R. R., and Parsons, J. T. (1991) *Mol. Cell. Biol.* **11,** 5113–5124
36. Zhan, X., Hu, X., Hampton, B., Burgess, W. H., Friesel, R., and Maciag, T. (1993) *J. Biol. Chem.* **268,** 24427–24431
37. Schuuring, E., Verhoeven, E., Litvinov, S., and Michalides, R. J. (1993) *Mol. Cell. Biol.* **13,** 2891–2898
38. Machesky, L. M. (2000) *J. Cell Biol.* **148,** 219–221
39. Pantaloni, D., Boujemaa, R., Didry, D., Gounon, P., and Carlier, M. F. (2000) *Nat. Cell Biol.* **2,** 385–391
40. Boujemaa-Paterski, R., Gouin, E., Hansen, G., Samarin, S., Le Clainche, C., Didry, D., Dehoux, P., Cossart, P., Kocks, C., Carlier, M. F., and Pantaloni, D. (2001) *Biochemistry* **40,** 11390–11404
41. Weaver, A. M., Heuser, J. E., Karginov, A. V., Lee, W. L., Parsons, J. T., and Cooper, J. A. (2002) *Curr. Biol.* **12,** 1270–1278
42. Zalevsky, J., Grigorova, I., and Mullins, R. D. (2001) *J. Biol. Chem.* **276,** 3468–3475
43. Takenawa, T., and Miki, H. (2001) *J. Cell Sci.* **114,** 1801–1809
44. Mizutani, K., Miki, H., He, H., Maruta, H., and Takenawa, T. (2002) *Cancer Res.* **62,** 669–674
45. Taunton, J., Rowning, B. A., Coughlin, M. L., Wu, M., Moon, R. T., Mitchison, T. J., and Larabell, C. A. (2000) *J. Cell Biol.* **148,** 519–530
46. Kaksonen, M., Peng, H. B., and Rauvala, H. (2000) *J. Cell Sci.* ***113 Pt*** **24,** 4421–4426
47. Frischknecht, F., and Way, M. (2001) *Trends Cell Biol.* **11,** 30–38
48. Suzuki, T., Miki, H., Takenawa, T., and Sasakawa, C. (1998) *EMBO J.* **17,** 2767–2776
49. Dehio, C., Prevost, M. C., and Sansonetti, P. J. (1995) *EMBO J.* **14,** 2471–2482
50. Higgs, H. N., and Pollard, T. D. (2000) *J. Cell Biol.* **150,** 1311–1320
51. Li, Y., Liu, J., and Zhan, X. (2000) *J. Biol. Chem.* **275,** 37187–37193
52. Goldberg, M. B., Barzu, O., Parsot, C., and Sansonetti, P. J. (1993) *J. Bacteriol.* **175,** 2189–2196
53. Zettl, M., and Way, M. (2001) *Nat. Cell Biol.* **3,** E74-E75
54. Blanchoin, L., Pollard, T. D., and Mullins, R. D. (2000) *Curr. Biol.* **10,** 1273–1282
55. Dayel, M. J., Holleran, E. A., and Mullins, R. D. (2001) *Proc. Natl. Acad. Sci. U. S. A.* **98,** 14871–14876
56. Le Clainche, C., Didry, D., Carlier, M. F., and Pantaloni, D. (2001) *J. Biol. Chem.* **276,** 46689–46692
57. Dancker, P., and Hess, L. (1990) *Biochim. Biophys. Acta* **1035,** 197–200
58. Volkmann, N., Amann, K. J., Stoilova-McPhie, S., Egile, C., Winter, D. C., Hazelwood, L., Heuser, J. E., Li, R., Pollard, T. D., and Hanein, D. (2001) *Science* **293,** 2456–2459
59. Robinson, R. C., Turbedsky, K., Kaiser, D. A., Marchand, J. B., Higgs, H. N., Choe, S., and Pollard, T. D. (2001) *Science* **294,** 1679–1684
60. Marchand, J. B., Kaiser, D. A., Pollard, T. D., and Higgs, H. N. (2001) *Nat. Cell Biol.* **3,** 76–82
61. Yamaguchi, H., Miki, H., Suetsugu, S., Ma, L., Kirschner, M. W., and Takenawa, T. (2000) *Proc. Natl. Acad. Sci. U. S. A.* **97,** 12631–12636
62. Zalevsky, J., Lempert, L., Kranitz, H., and Mullins, R. D. (2001) *Curr. Biol.* **11,** 1903–1913
63. Gouin, E., Gantelet, H., Egile, C., Lasa, I., Ohayon, H., Villiers, V., Gounon, P., Sansonetti, P. J., and Cossart, P. (1999) *J. Cell Sci.* **112,** 1697–1708
64. Huang, C., Ni, Y., Wang, T., Gao, Y., Haudenschild, C. C., and Zhan, X. (1997) *J. Biol. Chem.* **272,** 13911–13915
65. Weed, S. A., and Parsons, J. T. (2001) *Oncogene* **20,** 6418–6434
66. Weed, S. A., Du, Y., and Parsons, J. T. (1998) *J. Cell Sci.* **111,** 2433–2443
67. Kinley, A. W., Weed, S. A., Weaver, A. M., Karginov, A. V., Bissonette, E., Cooper, J. A., and Parsons, J. T. (2003) *Curr. Biol.* **13,** 384–393